Geologic and physiographic controls on bed-material yield, transport, and channel morphology for alluvial and bedrock rivers, western Oregon

Jim E. O'Connor[1,†], Joseph F. Mangano[1,2], Scott W. Anderson[1,3], J. Rose Wallick[1], Krista L. Jones[1], and Mackenzie K. Keith[1]

[1]*U.S. Geological Survey, Oregon Water Science Center, 2130 SW 5th Avenue, Portland, Oregon 97201, USA*
[2]*Department of Geosciences, Colorado State University, Fort Collins, Colorado 80523, USA*
[3]*Department of Geography, University of Colorado–Boulder, Boulder, Colorado 80309, USA*

ABSTRACT

The rivers of western Oregon have diverse forms and characteristics, with channel substrates ranging from continuous alluvial gravel to bare bedrock. Analysis of several measurable morphologic attributes of 24 valley reaches on 17 rivers provides a basis for comparing nonalluvial and alluvial channels. Key differences are that alluvial reaches have greater bar area, greater migration rates, and show systematic correlation among variables relating grain size to bed-material transport capacity. We relate these differences between channel types to bed-material transport rates as derived from a coupled regional analysis of empirical sediment yield measurements and physical experiments of clast attrition during transport. This sediment supply analysis shows that overall bed-material transport rates for western Oregon are chiefly controlled by (1) lithology and basin slope, which are the key factors for bed-material supply into the stream network, and (2) lithologic control of bed-material attrition from in-transport abrasion and disintegration. This bed-material comminution strongly affects bed-material transport in the study area, reducing transport rates by 50%–90% along the length of the larger rivers in the study area. A comparison of the bed-material transport estimates with the morphologic analyses shows that alluvial gravel-bed channels have systematic and bounding relations between bed-material transport rate and attributes such as bar area and local transport capacity. By contrast, few such relations are evident for nonalluvial rivers with bedrock or mixed-bed substrates, which are apparently more influenced by local controls on channel geometry and sediment supply. At the scale of western Oregon, the physiographic and lithologic controls on the balance between bed-material supply and transport capacity exert far-reaching influence on the distribution of alluvial and nonalluvial channels and their consequently distinctive morphologies and behaviors—differences germane for understanding river response to tectonics and environmental perturbations, as well as for implementing effective restoration and monitoring strategies.

INTRODUCTION

The rivers of western Oregon have channel beds ranging from fully alluvial to bedrock. A local history of in-stream gravel mining in conjunction with an ongoing permitting process for continued mining have prompted a series of investigations of bed-material production, transport, and channel morphology across this spectrum of channel types in western Oregon (Wallick et al., 2010, 2011; Jones et al., 2011, 2012a, 2012b, 2012c). These studies, expanded upon and synthesized here, show the importance of (1) geologic and physiographic controls on bed-material production and in-stream gravel flux; and (2) the differences between fully alluvial channels and those that locally flow on bedrock in terms of predicting transport rates, bed-material characteristics, and channel morphology.

Alluvial, Bedrock, and Mixed-Bed Channels

The distinction between alluvial and bedrock channels has broad implications regarding long-term channel incision (Howard, 1980; Whipple, 2004; Turowski et al., 2008a, 2008b; Turowski, 2012), channel morphology (Montgomery et al., 1996; Montgomery and Buffington, 1997; Tinkler and Wohl, 1998), and physical habitat (Stanford and Ward, 1993; Yarnell et al., 2006). Most fundamentally, the distinction relates to the balance between bed-material supply and river transport capacity (Gilbert, 1877, 1914; Howard, 1980; Whipple, 2004). Rivers in which the long-term channel transport capacity exceeds bed-material supply (termed supply- or detachment-limited rivers) will typically flow over bedrock beds for part or much of their courses. Where supply meets or exceeds transport capacity (transport-limited rivers), channel beds are typically formed of a continuous mantle of alluvial-bed material.

This categorization, however, masks substantial complexity. As summarized by Church (2002, 2006) and Lisle (2012), the morphology and transport conditions of alluvial channels involve interrelations among flow, channel and valley characteristics, sediment supply, and sediment grain size. These interrelations commonly create conditions of bed-material flux, channel form, bed elevation, and bed-sediment textures such that the bed material entering the system is balanced, at decadal to millennial time scales, by that exiting, i.e., the graded river of Mackin (1948). This system, classically depicted by the Lane-Borland balance between stream energy and sediment flux (Lane, 1955), has been subject to more than a century of scrutiny because of the many pragmatic implications of predicting alluvial channel behavior and morphology in consequence of changing environmental conditions.

Channels with bedrock beds and margins have also been studied extensively, but chiefly for their broad role in pacing valley incision and landscape evolution (summarized by Turowski, 2012). Finer-scale studies have mostly focused on bedrock channel forms (summarized by Wohl, 1998; Whipple, 2004; Richardson and Carling, 2005), erosional processes (Whipple et al., 2000; Wohl and Merritt, 2001; Johnson and Whipple, 2007; Goode and Wohl, 2010a), and transport conditions (Goode and Wohl, 2010b;

[†]E-mail: oconnor@usgs.gov

GSA Bulletin; March/April 2014; v. 126; no. 3/4; p. 377–397; doi:10.1130/B30831.1; 11 figures; 4 tables; Data Repository item 2014049; Published online 7 January 2014.

Hodge et al., 2011). Few "bedrock" channels, however, have continuous bedrock beds; most have patches, locally extensive, of alluvium in and flanking the channel, leading to the terms "mixed-bed" or "semi-alluvial" channels (Howard, 1980, 1998; Lisle, 2012; Turowski, 2012). The degree of alluvial cover has been hypothesized to modulate bedrock erosion (Gilbert, 1877; Sklar and Dietrich, 2001; Finnegan et al., 2007; Turowski et al., 2007). Only recently, however, have studies focused on the alluvial characteristics of channels that locally or continuously flow on bedrock (Chatanantavet and Parker, 2008; Goode and Wohl, 2010b; Hodge et al., 2011).

In this study, we directly compare alluvial and bedrock channels of western Oregon, and we relate their distribution and character to basic controls on bed-material flux and transport capacity. These differences and distinctions have implications for understanding river response to tectonics and environmental perturbations, as well as for implementing effective restoration and monitoring strategies.

Western Oregon Study Area and Analysis Summary

This synthesis derives from studies of several individual rivers and river basins in western Oregon. We have investigated channel conditions and bed-material transport rates for the Chetco and Umpqua River basins of southwestern Oregon (Wallick et al., 2010, 2011). Additionally, we have completed reconnaissance evaluations of Hunter Creek (Jones et al., 2011), Rogue River basin (Jones et al., 2012a), Coquille River basin (Jones et al., 2012b), and the five rivers entering Tillamook Bay and the Nehalem River (Jones et al., 2012c) (Fig. 1). In total, these studies encompass 17 rivers in western Oregon (Table 1).

All of these main-stem rivers drain into the Pacific Ocean or estuarine bays (Fig. 1). The Rogue and Umpqua Rivers, the largest of the study area at 13,390 km^2 and 12,103 km^2, respectively (Table 1), have sources in the Cascade Range of southern Oregon; the others begin in the Coast Range or Klamath Mountains of western Oregon and northwestern California. The Hunter Creek basin, with a drainage area of 115 km^2, is the smallest for which we have detailed measurements. All of these rivers are subject to the cool and wet maritime climate of the Pacific Northwest. All have been affected to some degree by the typical Pacific Northwest land-use perturbations such as dams, timber harvest (and splash-damming), fire, in-stream and floodplain gravel mining, placer mining, and local channel and floodplain development.

The regional geology is important to our analysis, and we have aggregated existing mapping into six main lithologic groupings (Fig. 1). The Paleozoic and Mesozoic rocks of the tectonically accreted Klamath terrane underlie much of the southwestern part of the study area. Uplifted Tertiary marine sediments constitute the Coast Range sedimentary province underlying much of the western part of the study area. Tertiary marine volcanic rocks within the Coast Range and the Columbia River Basalt Group in the northern part of the study area have been grouped together into what we term the Coast Range volcanics province. The axis of the Cascade Range is underlain by Quaternary volcanic rocks of the High Cascades province, and these rocks are flanked to the east and west by Tertiary volcanic rocks grouped into the Western Cascades lithologic province. Basins, broad valleys, and coastal plains are underlain by Quaternary sediment.

Our analysis is based on morphologic observations from 24 valley reaches within the 17 rivers. Analyzed reaches span the spectrum of fully alluvial to bedrock (Fig. 2). Our measurements of channel and bar area, channel migration rates, channel slope, and bar sediment texture are evaluated with respect to (1) field-based assessment of their alluvial versus bedrock character, and (2) estimates of local mean annual bed-material flux. Local bed-material flux is derived from a regional empirical analysis of bed-material production paired with a separate experiment-based analysis of bed-load clast comminution. We test these estimated bed-material fluxes against several independent assessments of bed-material supply and transport. We then discuss the specific implications of these results, first by comparing the Rogue and Umpqua Rivers, and then by broader regional assessment and comparison of the distribution and morphology of alluvial and nonalluvial valley reaches. Finally, we develop broader inferences regarding overall physiographic and geologic controls on the distribution of alluvial and nonalluvial channels, concluding with management implications.

MORPHOLOGICAL ANALYSIS—METHODS AND RESULTS

The morphologic measurements enable assessment of the regional variety of rivers and controls on their characteristics. The valley reaches (Table 1) were defined by the studies of Wallick et al. (2010, 2011) and Jones et al. (2011, 2012a, 2012b, 2012c) and include the contiguous portions of the 17 rivers in which the channel beds are composed of, or are locally flanked by, substantial accumulations of modern alluvium. All of these reaches have gradients less than 0.005 and would be considered transport or response reaches in the Montgomery and Buffington (1997) categorization. Study reaches were defined on the basis of broad-scale geomorphic characteristics, with boundaries typically corresponding to major confluences, changes in valley confinement, and extent of tidal influence. The 24 separate reaches summarized here do not include the tidal reaches identified in these previous studies. The short fluvial reaches of Hunter Creek and the Chetco, Wilson, and Miami Rivers defined in our previous studies (Wallick et al., 2010; Jones et al., 2011, 2012c) have been aggregated in this assessment so that each one of these rivers is represented by single valley reaches. The resulting 24 study reaches range from <5 km to as long as 115.7 km (Table 1). The Umpqua and Rogue River basins have the most reaches, reflecting distinct morphological differences along these large and long rivers and their major tributaries, while several of the shorter coastal rivers each consist of a single reach. All of the study reaches have gravel bed material.

Valley Reach Classification

Each reach was defined as alluvial or nonalluvial solely on the basis of the presence or absence of continuous alluvial cover on the channel bed as evident from aerial photographs (Table DR1[1]) and field observations (Fig. 2; Table 1). In accordance with Lisle's (2012) identification of this critical threshold condition, reaches in which patches of in-channel bedrock were exposed to sufficient extent to locally control the river profile were judged nonalluvial. Most of the nonalluvial reaches are "mixed bed" or "semi-alluvial" in the terminology of Howard (1998) and Lisle (2012). For two reaches, the North Umpqua River and the Coast Range reach of the main-stem Umpqua River, the channel flows on bedrock for the majority of its length (Fig. 2C). These reaches probably meet most workers' definitions of bedrock channels. While the distinction between "bedrock" and "mixed bed" somewhat arbitrarily subdivides the 12 nonalluvial reaches, the other 12 reaches classified as "alluvial" were distinctive in that they all had continuous alluvial cover on their beds. Because some of the alluvial reaches were locally confined by bedrock margins, they would be classified as bedrock rivers by Turowski et al. (2008b), but their delineation as alluvial in this study reflects the pragmatic considerations from

[1]GSA Data Repository item 2014049, supplementary tables and figures, is available at http://www.geosociety.org/pubs/ft2014.htm or by request to editing@geosociety.org.

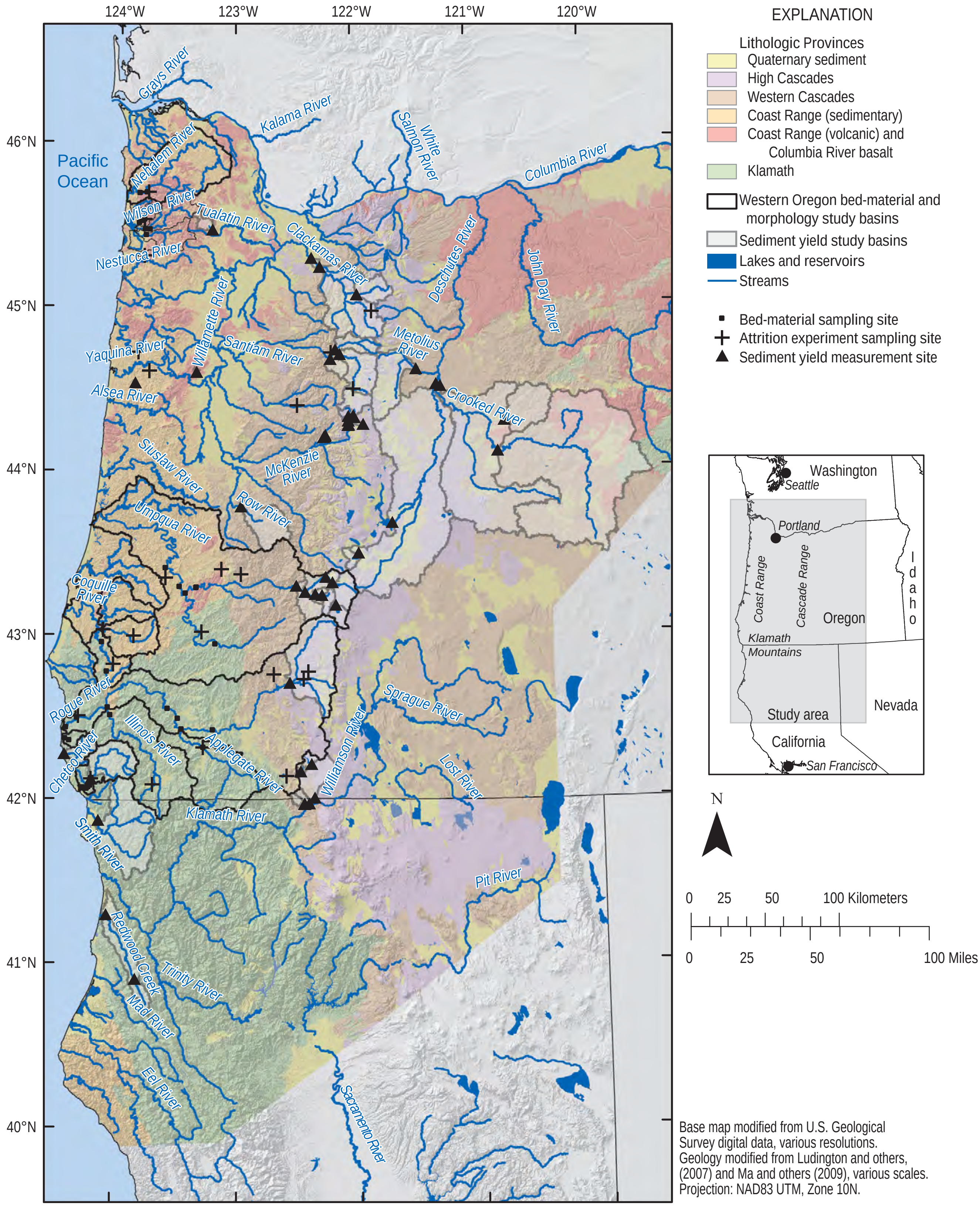

Figure 1. Regional map showing grouped lithologic units, sediment yield measurement sites and contributing basins, sample locations for attrition experiments, and basin boundaries for the western Oregon gravel transport and channel morphology studies of Wallick et al. (2010, 2011) and Jones et al. (2011, 2012a, 2012b, 2012c). Specific site locations are provided in supplementary Tables DR2, DR3, and DR8 (see text footnote 1). Lithologic groupings are provided in supplementary Table DR7 (see text footnote 1).

TABLE 1. SUMMARY OF ANALYSIS REACHES

River	Reach name	Centerline reach length (km)	Drainage area (km²)*	Average floodplain width (m)	Average wetted width (m)	Sinuosity (m/m)	Reach slope (m/m)†	Total bar area (km²)	Migration rate (m/yr)§	Average annual discharge (m³/yr)#	Bed-material flux (including attrition) (t/yr)**
Alluvial reaches											
Chetco	Chetco	12.2	900	336	51	1.10	0.00126	0.63	3.8	2.01×10^9	111,226
Hunter Creek	Hunter	12.4	110	175	18	1.19	0.00210	0.24	1.1	N.D.††	8552
Applegate	Lower Applegate	41.6	1990	651	33	1.18	0.00280	2.97	3.2	6.29×10^8	120,292
Illinois	Illinois	6.5	2560	225	55	1.09	0.00190	0.60	1.0	3.66×10^9	272,843
Rogue	Lobster Creek	37.2	13,310	261	95	1.07	0.00070	2.35	1.9	8.79×10^9	444,404
S. Fk. Coquille	Broadbent	30.7	640	356	24	1.31	0.00092	0.35	1.4	6.91×10^8	21,462
Wilson	Wilson	4.0	494	823	33	1.26	0.00124	0.14	1.2	1.05×10^9	25,352
Miami	Miami	9.3	86	256	13	1.14	0.00402	0.13	1.4	N.D.††	9949
Tillamook	Tillamook	10.2	110	369	14	1.24	0.00220	0.03	0.6	N.D.††	3396
Trask	Trask	5.1	424	768	29	1.18	0.00160	0.09	0.7	8.73×10^8	15,146
Kilchis	Kilchis	10.3	167	454	26	1.32	0.00146	0.05	1.1	N.D.††	23,426
Nehalem	Nehalem	6.8	1840	314	51	1.06	0.00129	0.13	1.4	2.37×10^9	34,692
Mixed-bed reaches											
Applegate	Upper Applegate	15.0	1370	422	26	1.06	0.00360	0.07	0.6	4.57×10^8	100,425
Rogue	Grants Pass	25.4	6470	721	69	1.04	0.00140	0.33	1.0	3.03×10^9	1919
Rogue	Merlin	20.3	8890	426	83	1.06	0.00140	0.98	1.4	3.65×10^9	132,007
Rogue	Galice	88.8	10,290	126	54	1.02	0.00200	0.94	1.1	5.12×10^9	225,962
S. Fk Coquille	Powers	18.5	490	92	23	1.06	0.00270	0.27	0.8	6.91×10^8	19,677
Md. Fk. Coquille	Bridge	15.4	800	110	24	1.07	0.00147	0.04	0.7	6.64×10^8	5061
N. Fk. Coquille	Gravelford	14.6	750	287	16	1.20	0.00031	0.01	0.6	8.35×10^8	1917
S. Umpqua	Days Creek	47.5	1960	480	32	1.10	0.00246	0.84	0.6	9.13×10^8	113,007
S. Umpqua	Roseburg	75.9	4660	783	56	1.22	0.00107	1.03	1.2	2.44×10^9	165,172
Umpqua	Garden Valley	18.8	8930	1196	83	1.15	0.00096	0.09	1.2	5.74×10^9	145,594
Bedrock reaches											
Umpqua	Coast Range	115.7	10,490	505	104	1.03	0.00081	0.59	N.D.	6.57×10^9	63,035
N. Umpqua	North Umpqua	47.0	3520	468	72	1.06	0.00186	0.32	N.D.	3.30×10^9	68,965

Note: Morphological characteristics were digitized from National Agriculture Imagery Program ortho-imagery from 2005 and 2009; image resolution and acquisition dates are provided in supplementary Table DR1 (see text footnote 1).

*Determined at downstream end of reach.

†Supplementary Table DR4 shows basis for reach-slope values (see text footnote 1).

§Centerline migration rate measured relative to floodplain axis for period 2005–2009; only calculated for alluvial and mixed-bed reaches.

#Mean annual discharge determined from U.S. Geological Survey gauging station records; supplementary Table DR5 (see text footnote 1).

**As determined for calculation point(s) representative for the reach; includes the effects bed-material trapping by dams; analysis area noted in supplementary Table DR2 (see text footnote 1).

††N.D.—not determined.

regulatory and geomorphic perspectives that (1) they can be categorized from field inspection and aerial photographs, (2) the channels could plausibly incise within decadal time scales in response to a reduction in bed-material supply or increase in transport capacity, and (3) bed-material transport is likely capacity limited and, consequently, can be reliably estimated by empirical flow-based sediment rating curves or by bed-material transport capacity relations.

Reach and Site Measurements

For each of the 24 reaches, we mapped and measured the low-flow wetted channel, channel centerline, and all exposed gravel bars with areas greater than 300 m² at a scale of 1:3000 using 0.5 and 1 m resolution ortho-imagery collected during summer low-flow periods in 2005 and 2009 by the National Agriculture Imagery Program (Fig. 3; Table 1; Tables DR1 and DR2 [see footnote 1]). Additionally, we mapped the geomorphic floodplain for each reach, defined as the lateral extent of Holocene-era fluvial processes, on the basis of available geology, soils, and topography and reconnaissance field inspection, as described in Wallick et al. (2011) for the Umpqua River. From this mapping, we evaluated 2005–2009 channel centerline migration rates relative to the floodplain centerline for the intervening period in the manner of O'Connor et al. (2003b).

Bed-material textures at 93 bars located in 19 of the study reaches were sampled during the summers of 2008–2010 (Table DR3 [see footnote 1]). For each sampling site, we employed a modified grid technique (Kondolf et al., 2003) to measure 200 surface clasts by template (Federal Interagency Sediment Project U.S. SAH-97 Gravelometer) at 0.3 m increments along two parallel 30 m tapes. Bed-material substrate was sampled at 45 of the surface-material sampling sites by removing the surface layer from a 1 m² area at the grid center and then collecting ~40–60 L of sediment, such that the largest particles did not constitute more than ~5% of the total sample volume. Most bed-material substrate samples were analyzed by the U.S. Geological Survey (USGS) Sediment Laboratory in Vancouver, Washington, where samples were dried and weighed in half-phi intervals. Some substrate samples, particularly those in the Galice valley reach of the Rogue River, were field sieved. Sampling sites were predominantly located at bar apices, though vegetation, bedrock outcrops, and other factors dictated that some bars were sampled at other locations. For sites in the Chetco and Umpqua River drainages, we also conducted partial lithologic classification of bed-material samples (Wallick et al., 2010, 2011).

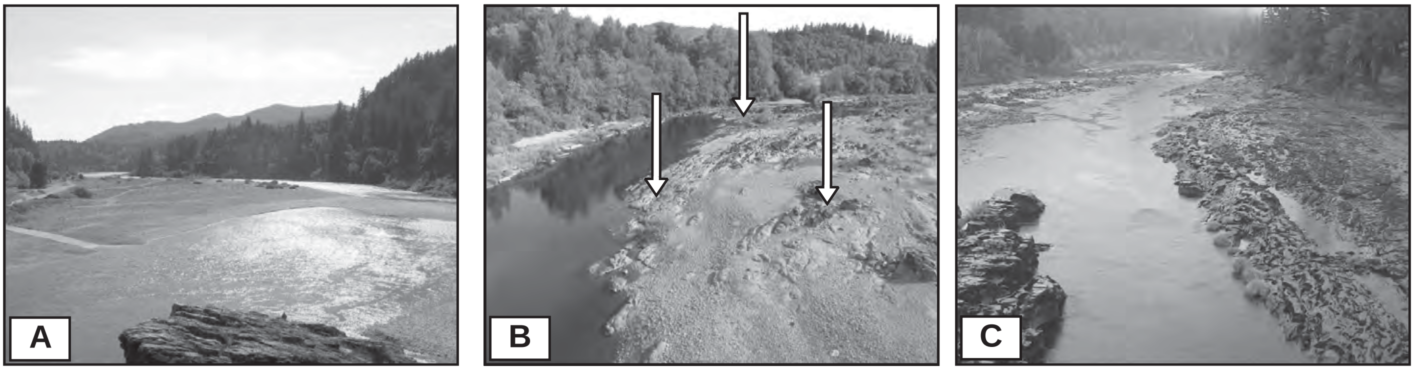

Figure 2. Photographs of alluvial, mixed, and bedrock rivers within the western Oregon study area. (A) View downstream of a portion of the Lobster Creek reach of the Rogue River. Channel flows over continuous alluvial gravel bed. (B) View upstream of a portion of the Roseburg reach of the South Umpqua River. Channel flows over a mixed bed of bedrock (indicated by arrows) and patchy gravel alluvium. (C) View upstream of a portion of the Coast Range reach of the Umpqua River where the bed is predominantly bedrock.

Channel slope was measured at both the reach scale and locally about each bed-material sampling site over a distance of 20 channel widths (Tables DR2 and DR4 [see footnote 1]). Elevation data underlying the slope calculations included light detection and ranging (LiDAR) topographic surveys, local thalweg and water-surface profile surveys, and elevation information from USGS 7.5 minute quadrangles (commonly in the form of USGS 10 m digital elevation models). For reaches in which gauging records existed or for which flow could be estimated from upstream and downstream gauges on the same river system (Table DR5 [see footnote 1]), we also determined the average annual water flow (Table 1).

General Patterns and Correlations

These observations and measurements enable empirical evaluation of regional patterns among channel morphology, channel migration, bed sediment texture, and flow conditions (Figs. 3 and 4). An evident factor from comparison among measured parameters is that many morphologic and texture characteristics are independent of the alluvial or nonalluvial character of the reach. Across both categories, slope varied from 0.0003 to 0.004, channel width varied from 13 m to 104 m, and floodplain width varied from 92 m to 1196 m, without significant differences between the alluvial and nonalluvial categories. Also, slope against drainage-area plots do not clearly discriminate between alluvial and nonalluvial reaches; they actually show that most of the nonalluvial reaches are associated with larger drainage areas (Fig. 4A), thereby contrasting with many other environments (Howard and Kerby, 1983; Montgomery et al., 1996; Massong and Montgomery, 2000).

The main obvious difference between alluvial and nonalluvial reaches is in bar area (Fig. 3D). Alluvial reaches have scaled bar areas (relative to low-flow channel area) of 0.35–2.16, with a mean of 0.83. By contrast, nonalluvial reaches have scaled bar areas of 0.03–0.59, with a mean of 0.24. For the analyzed reaches, a scaled-bar-area criterion of 0.3 would have correctly classified 21 of the 24 reaches into alluvial or nonalluvial categories.

Centerline migration rates were also generally greater for the alluvial reaches. The migration rates for alluvial channels, scaled by the reach-average low-flow channel width, ranged from 0.02 yr^{-1} to 0.11 yr^{-1} (mean 0.05 yr^{-1}) for the 2005–2009 period, compared to <0.02 yr^{-1} to 0.04 yr^{-1} (mean 0.02 yr^{-1}) for the nonalluvial reaches (Fig. 3E). The two alluvial reaches with the lowest migration rates, the Illinois River and the Lobster Creek reach of the Rogue River, are both closely confined by valley margins (Fig. 3B), probably inhibiting lateral migration.

Median particle diameter (D_{50}) for the 93 bar surfaces ranged from 12 to 205 mm (Fig. 3F; Table DR3 [see footnote 1]). In general, the nonalluvial reaches had coarser bars (two-sample *t*-test; $p = 0.023$). Grain size on nonalluvial reaches was weakly but significantly correlated with local slope ($R^2 = 0.18$; $p < 0.001$),[2] whereas no such correlation was shown by the alluvial reaches (Fig. 4B). Armoring (ratio of surface D_{50} to subsurface D_{50}) varied from 1 to 5.5 among the 45 sites for which subsurface samples were collected, but with no evident difference between the alluvial and nonalluvial reaches (Fig. 3F).

In the absence of local hydraulic information, a measure of local transport capacity relative to grain size, D^*, was calculated on the basis of the nondimensional formulation,

$$D^* = (W{\cdot}S)/D_{50}, \tag{1}$$

where W is reach-averaged wetted width at low flow (Table 1), D_{50} is the median bar-surface grain size, and S is local slope measured at each bed-material sampling site (Table DR3 [see footnote 1]). Because channel width presumably scales with flow depth, D^* is analogous to the dimensionless shear stress variable known as the Shields number, τ^*,

$$\tau^* = (\rho g d S)/[(\rho_s - \rho) g D], \tag{2}$$

where ρ is fluid density, ρ_s is clast density, g is gravitational acceleration, d is flow depth, and D is a characteristic particle diameter such as D_{50}. These formulations show that τ^* and D^* both essentially express the ratio of fluid shear stress on bed-material particles to particle weight.

For alluvial rivers in steady state, where transport capacity and grain size interact in relation to sediment supply (Mackin, 1948; Lane, 1955) to maintain steady transport conditions, D^* should correlate with measures of sediment supply, such as bar area (Fig. 4C). Conversely for nonalluvial rivers, the generally higher values of D^* and the absence of correlation are consistent with these nonalluvial reaches having transport capacities in excess of bed-material sediment supply.

A correlation involving all reach types is that of bar area with channel migration rate (Fig. 4D), with the alluvial reaches generally having both greater bar areas and migration rates. This finding accords with active bar formation and lateral channel movement being highly interrelated processes (Church, 1992). The bar-rich but laterally confined Illinois River is a distinct outlier.

Taken together, plan-view morphologic and bed-texture characteristics of Oregon coastal

[2]All correlations are based on linear regression of log-transformed values, with $p \leq 0.05$ judged significant for scaling coefficients.

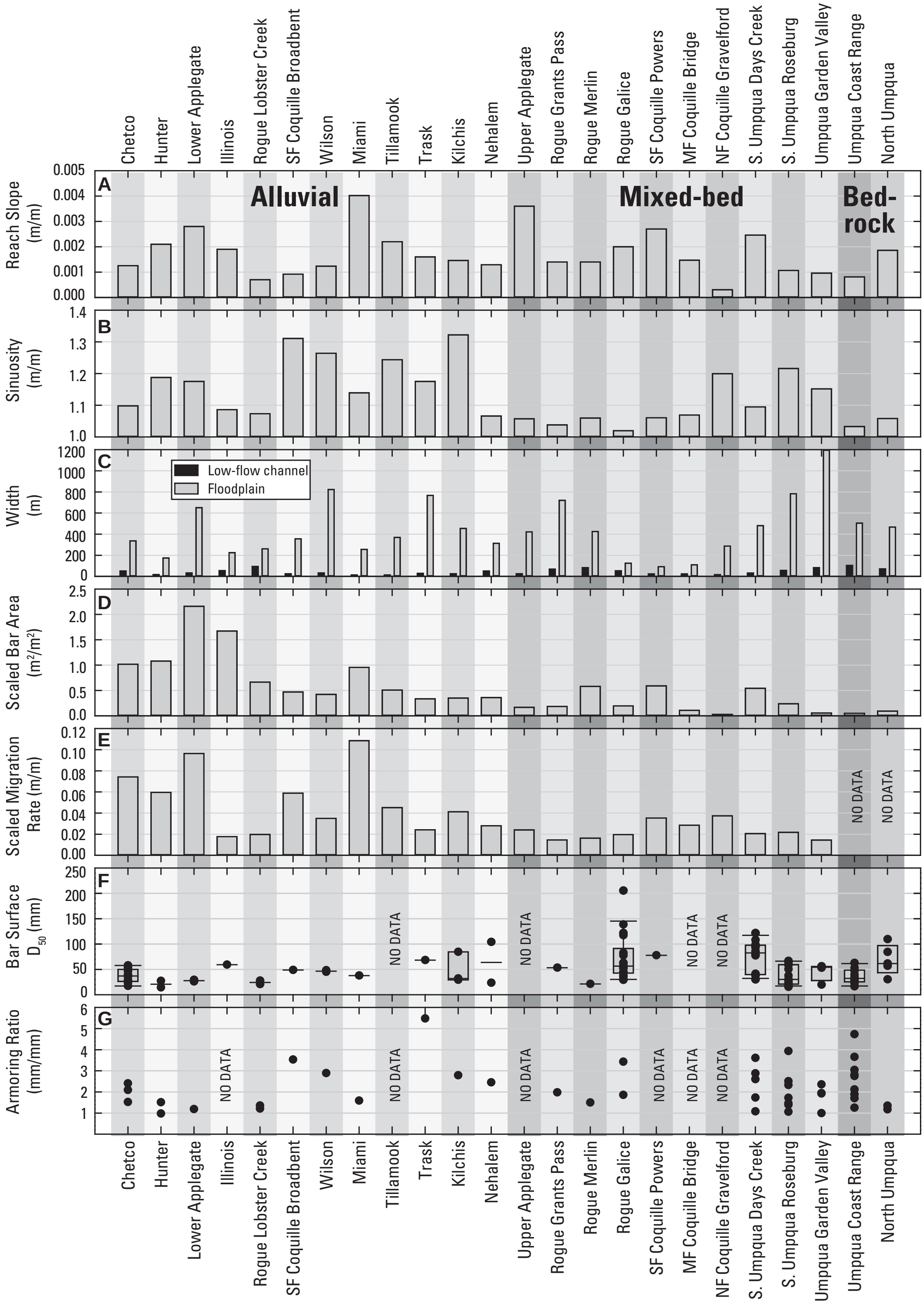

Figure 3. Summary plots of morphologic attributes of the 24 study reaches, categorized into alluvial, mixed bed, and bedrock. Box plots for the bar-surface grain-size measurements show distribution of median grain-size values for valley reaches for which we made multiple measurements. Reaches in each category are ordered south to north. Boxes indicate median, 25th, and 75th percentile values, with attached whiskers indicating 10th and 90th percentile values. Supporting data are tabulated in supplementary Tables DR2 and DR3 (see text footnote 1).

rivers span a wide range of conditions. Some aspects, particularly bar area, particle size, and migration rates, appear to differ between a priori defined transport-limited alluvial and supply-limited nonalluvial (mixed-bed and bedrock) reaches. Other characteristics, such as slope, channel width, and channel confinement, show little relation to alluvial or nonalluvial status. For the alluvial rivers in the study area, indicators of bed-material transport rates, such as channel migration rate and transport capacity (as measured by D^*), are strongly correlated with bar area, as would be expected for transport-limited systems.

All of these observations and relations, however, are in the absence of information on actual bed-material transport rates. Consequently, we expand the analysis by developing reach-specific estimates of annual bed-material transport from regional measurements of bed-material supply and transport in combination with estimates of particle comminution during fluvial transport.

BED-MATERIAL TRANSPORT—METHODS AND RESULTS

We combine a regional analysis of bed-material supply with experiments on clast comminution to give spatially explicit determinations of average annual bed-material flux for the rivers of the study area. For this analysis, we define bed material as clasts of 0.5 mm diameter and greater, consistent with d_{16} of the 45 sampled bar substrates ranging from 0.6 to 28 mm (median 1.6 mm) (Table DR3 [see footnote 1]). We assume steady-state conditions—meaning no net changes in storage—and describe average annual conditions for all aspects of the analysis, recognizing that some features of these fluvial systems reflect historical conditions and processes and that actual transport conditions vary tremendously from year to year.

Bed-Material Yield

Bed material entering the fluvial network was estimated from empirical relations between measured bed-material flux and physiographic, geologic, and climatic properties of contributing basins. The approach is similar to the sediment yield studies of Hooke (2000), O'Connor et al. (2003a), and Aalto et al. (2006), although it focuses on bed material (grain size > 0.5 mm) rather than total clastic yield.

From existing literature, we assembled 34 observations of bed-material transport in rivers of western Oregon and northern California from which we could derive annual transport rates (Table 2; Table DR6 [see footnote 1]). The majority of these were derived from reservoir or catch-basin surveys, but some sites, such as Oak Creek, Chetco River, and Smith River, were based on bed-load sampling in combination with either a sediment rating curve or application of bed-load transport equations. These bed-material yield measurements were derived from basins ranging from 0.6 km^2 to 6906 km^2 (median area 230 km^2) and represented durations of 1–95 yr. Contributing areas were adjusted for the presence of upstream dams. We did not use data from landslide surveys or other similar indirect approaches for estimating basin yield or in-stream bed-material transport.

These measurements have considerable uncertainty. Because of the difficulty and uncertainty in measuring bed load, and then extrapolating to estimate annual loads (Gomez,

Figure 4. Scatter plots of selected morphologic and grain-size observations for alluvial, mixed-bed, and bedrock channels in western Oregon study area. Supporting data are tabulated in supplementary Tables DR2 and DR3 (see text footnote 1). (A) Slope-area plot. The absence of clear separation between alluvial and nonalluvial reaches, and the preponderance of nonalluvial reaches with relatively larger drainage areas are strong evidence that factors besides flow and channel slope control the distribution of alluvial and nonalluvial reaches. (B) Median grain size of bar-surface particle counts in relation to channel slope, showing a significant ($P < 0.001$) positive correlation (and 95% confidence limits) between slope and grain size for mixed-bed and bedrock channels. No such correlation is evident for alluvial channels. This plot has more points than the other ones of this figure because some valley reaches had several grain-size measurements, with local slope determined for each measurement site. (C) Scaled bar area (normalized by low-flow channel area) with respect to D^* (= $[W{\cdot}S]/D_{50}$), a measure of local transport capacity relative to grain size, showing significant positive correlation among alluvial channels. Horizontal uncertainty bars show standard deviation of reach observations where five or more measurements were made, and entire range for reaches with fewer bar-surface grain-size measurements. No uncertainty bars indicate only a single measurement for the reach. (D) Relation of scaled bar area to migration rate (scaled by mean channel width), showing significant positive correlation among all study reaches.

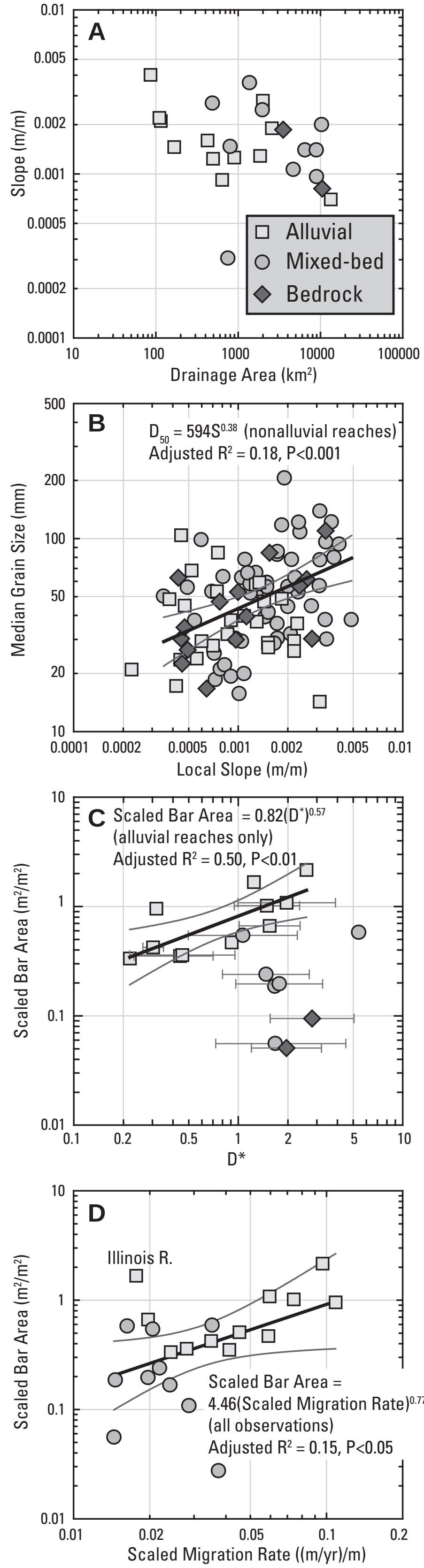

TABLE 2. SUMMARY OF REGIONAL BED-MATERIAL YIELD OBSERVATIONS

River and measurement site	Location UTM, Zone 10N Easting (m)	Location UTM, Zone 10N Northing (m)	Contributing area (km²)	Measurement method	Bed-material yield (t/km³/yr)	Included in regression model	Included in residual analysis	Source
Scoggins Creek, Henry Hagg Lake, Willamette basin	484,376	5,035,509	100.4	Reservoir survey	50.4	No	Yes	Ferrari (2001)
Clackamas River, River Mill Reservoir	550,928	5,016,366	1761.1	Reservoir survey	31.0	Yes	Yes	Wampler (2004)
Clackamas River, North Fork Reservoir	556,542	5,010,243	1390.3	Reservoir survey	98.5	Yes	Yes	Wampler (2004)
Clackamas River, Harriet Lake	581,420	4,991,735	337.4	Reservoir survey	4.6	Yes	Yes	Wampler (2004)
Breitenbush River, Brightenbush Arm, Santiam basin	567,055	4,954,424	279.8	Reservoir delta survey	12.8	No	Yes	Tetratech (2009)
Santiam River, Santiam Arm, Detroit Reservoir	563,779	4,947,892	572.7	Reservoir delta survey	10.1	No	Yes	Tetratech (2009)
Blowout Creek, Blowout Arm, Santiam basin	563,779	4,947,892	136.9	Reservoir delta survey	21.6	No	Yes	Tetratech (2009)
Metolius River, Metolius arm, Lake Billy Chinook, Deschutes basin	621,607	4,941,628	822.2	Reservoir delta survey	7.2	Yes	Yes	J.E. O'Connor, personal observation (1998)
Oak Creek, Willamette basin	473,558	4,939,125	7.2	Bed-load sampling/rating	12.9	Yes	Yes	P. Klingeman, Oregon State University (2009, written commun.)
Flynn Creek, Alsea River basin	432,228	4,932,084	2.1	Bed-load sampling/rating	14.7	Yes	Yes	Stednick (2008)
Deschutes River, Deschutes River arm, Lake Billy Chinook	635,126	4,931,722	5597.7	Reservoir delta survey	2.2	Yes	Yes	O'Connor et al. (2003a)
Crooked River, Crooked River arm, Lake Billy Chinook, Deschutes basin	637,827	4,930,421	4166.6	Reservoir delta survey	1.5	Yes	Yes	O'Connor et al. (2003a)
Ochoco Creek, Ochoco Reservoir, Deschutes basin	681,318	4,907,510	755.3	Reservoir survey	16.1	Yes	Yes	O'Connor et al. (2003a)
Smith River, Smith Reservoir, McKenzie basin	576,020	4,906,259	45.7	Reservoir survey	50.2	Yes	Yes	Stillwater Sciences (2006)
McKenzie River, Trail Bridge Reservoir, McKenzie arm, McKenzie basin	576,258	4,903,592	42.1	Reservoir survey	4.0	Yes	Yes	Stillwater Sciences (2006)
Smith River, Trail Bridge Reservoir, Smith Arm, McKenzie basin	575,790	4,903,240	13.7	Reservoir survey	54.6	Yes	Yes	Stillwater Sciences (2006)
HJ Andrews watershed 1, McKenzie basin	560,469	4,896,480	1.0	Bed-load sampling/rating	3.0	No	No	Grant and Wolff (1990)
HJ Andrews watershed 2, McKenzie basin	560,341	4,895,714	0.6	Bed-load sampling/rating	9.0	No	No	Grant and Wolff (1990)
HJ Andrews watershed 3, McKenzie basin	559,280	4,895,185	1.0	Bed-load sampling/rating	14.0	No	No	Grant and Wolff (1990)
Crooked River, Prineville Reservoir, Deschutes basin	677,007	4,886,604	6906.4	Reservoir survey	5.2	Yes	Yes	O'Connor et al. (2003a)
Row River, Dorena Reservoir, Willamette basin	503,611	4,848,181	686.0	Reservoir survey	21.6	No	Yes	Ambers (2001)
North Umpqua River, Lemolo No. 2 Diversion Dam	560,803	4,800,514	64.1	Reservoir survey	11.7	Yes	Yes	Stillwater Sciences (2000)
North Umpqua River, Lemolo Lake	565,285	4,796,890	310.3	Reservoir survey	57.9	No	Yes	Stillwater Sciences (2000)
North Umpqua River, Soda Springs Reservoir	540,923	4,794,574	259.1	Reservoir survey	54.0	Yes	Yes	Stillwater Sciences (2000)
North Umpqua River, Toketee Lake	546,783	4,790,324	200.3	Reservoir survey	48.0	Yes	Yes	Stillwater Sciences (2000)
Clearwater River, Clearwater forebays 1 and 2, North Umpqua basin	553,733	4,788,914	48.5	Reservoir survey	20.5	Yes	Yes	Stillwater Sciences (2000)
Clearwater River, Stump Lake, North Umpqua basin	558,333	4,788,317	104.1	Reservoir survey	24.6	No	Yes	Stillwater Sciences (2000)
Rogue River, Lost Creek Lake (reservoir)	536,630	4,728,934	1658.1	Reservoir delta survey	14.4	Yes	Yes	Dykaar and Taylor (2009)
Chetco River	401,893	4,664,115	701.9	Bed-load sampling/equations	220.5	Yes	Yes	Wallick et al. (2010)
Jenny Creek, Iron Gate Reservoir, Klamath basin	549,796	4,647,406	441.0	Reservoir delta survey	4.0	Yes	Yes	PacifiCorp (2004)
Camp/Dutch and Scotch Creeks, Iron Gate Reservoir, Klamath basin	546,483	4,647,026	97.7	Reservoir delta survey	25.1	Yes	Yes	PacifiCorp (2004)
Smith River, California	406,729	4,636,267	1726.5	Bed-load sampling/equations	108.7	Yes	Yes	MFG Inc. et al. (2006)
Redwood Creek at Orick, 1945–1991	412,017	4,572,477	717.3	Bed-load sampling/rating	364.8	No	No	Lisle and Madej (1992)
Redwood Creek at Blue Lake, 1945–1991	431,345	4,528,678	174.8	Bed-load sampling/rating	435.6	No	No	Lisle and Madej (1992)

Note: Complete information on derivation of mass estimates, period of record, and predictor variable values is provided in supplementary Table DR6 (see text footnote 1).

1991), values based on bed-load measurement programs are optimistically accurate to within a factor of two in the best of circumstances, such as for the Chetco River (Wallick et al., 2010). Uncertainties in estimating bed-material from the reservoir surveys may be even greater, owing to survey errors and uncertainties in addition to assumptions or limited knowledge of deposit volume density, the component of the deposit that is bed material, and reservoir trap efficiency.

Our empirical analysis was premised on basin factors such as physiography, climate, and geology being the major factors controlling bed-material supply to the fluvial system. Similar to the analyses O'Connor et al. (2003a) and Aalto et al. (2006), potential physiographic and climatic predictor variables were calculated for the contributing area of each measurement location (Table 2; Table DR6 [see footnote 1]). Also, for each contributing area, a categorical variable of dominant geology was determined from the classification of regional lithologies (Fig. 1; Table DR7 [see footnote 1]), with dominance defined as the geologic unit of greatest spatial extent.

The resulting best-fit power-law model (Fig. 5) predicts unit bed-material yield as a function of average basin slope and the presence or absence of Klamath terrane rocks as the dominant lithologic unit,

$$Q_{bm} = 450 \cdot S^{2.2727} \times 10^{(0.356 \cdot KT)}, \qquad (3)$$

where Q_{bm} is annual unit bed-material flux in tonnes (t) per square kilometer per year, S is mean basin slope (dimensionless, derived from USGS 1/3 arc-second resolution topographic data), and KT represents the categorical variable of the dominant lithologic unit, for which the value equals 1 if the dominant lithology is the Klamath terrane and equals 0 for all other dominant lithologic units. The model coefficient has been adjusted by a factor of 1.145, using the "smearing estimate of bias" associated with the distribution of residuals to account for the prediction bias resulting from back transformation from logarithmic units (Newman, 1993). The overall result is easily interpretable in that bed-material yield is everywhere strongly related to basin slope, and that bed material yield is ~2.3 times greater when the dominant lithology of the basin is Klamath terrane rocks, which probably reflects its more intense deformation history compared to the other lithologic groups.

This relation was strengthened by judicious removal of outliers (Fig. 5; Table DR6 [see footnote 1]). Five outliers had clear reasons for removal from the analysis. In particular, the two Redwood Creek measurements were from

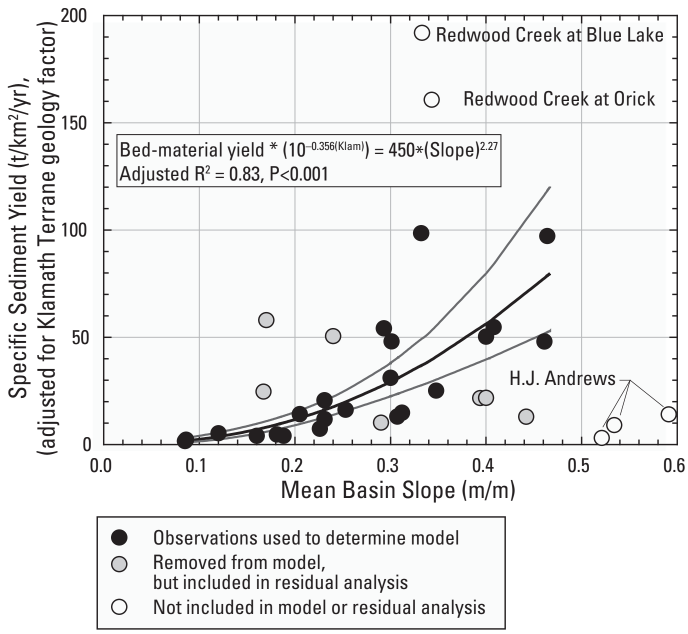

Figure 5. Bed-material yield observations and selected power-law model (and 95% confidence limits). Yield values are adjusted for Klamath terrane geology factor to enable plotting against mean basin slope of contributing watershed. Measurement site information, references, and all values are given in Table 2 and supplementary Table DR6 (see text footnote 1).

highly disturbed watersheds where sediment fluxes have been historically higher than natural (Nolan and Janda, 1995). The three low yields from the H.J. Andrews Experimental Forest are from very small (1 km^2 or less) and densely forested watersheds for which the short measurement periods did not include any significant mass movements, which episodically contribute bed-material sediment in these watersheds. Seven additional observations were removed from the regression analysis on the basis of being visual outliers and derived from less reliable measurements, but these were retained in the analysis of residuals.

The final regression model was based on the 22 retained observations and had a coefficient of determination (R^2) value of 0.83 (P < 0.001). Both the slope coefficient and Klamath variable scaling factor have P values less than 0.1. Residuals, including the visual outliers, are uncorrelated with other trial parameters, with the exception of drainage density (Table 3; Fig. DR1 [see footnote 1]). While drainage density was positively correlated with total sediment yield for the Deschutes River basin in central Oregon (O'Connor et al., 2003a), the correlation in this analysis is negative with this larger data set, and it is driven by the visual outliers not used in the final regression. Moreover, its inclusion reduces the significance of the Klamath variable and the overall model. Consequently, we judge the model based on slope and the presence or absence of Klamath terrane rocks (Fig. 5) as the best overall model for predicting bed-material yield in western Oregon with the available bed-material flux information.

The results of this sediment yield analysis for western Oregon are very similar to those of Aalto et al. (2006) for the Bolivian Andes, where multiple regression analyses involving several similar predictor variables resulted in a final model in which slope and geology explained 90% of the variance in sediment yield in the Bolivian Andes. These results also concur with an earlier analysis the Deschutes River basin (which includes some of the data used in this analysis), in which sediment yield was strongly correlated to basin slope and drainage density, which in turn correlated to local geologic units (O'Connor et al., 2003a).

Bed-Material Comminution

The bed-material yield analysis provides a means of estimating the mass of bed material entering the fluvial system. However, bed material moving downstream is constantly diminished by particle attrition or comminution. Although particle breakage and abrasion do not reduce the total sediment flux, these processes transform bed material into size fractions small enough to be transported in suspension. Such comminution likely contributes to the common observation of downstream fining of bed material in many fluvial systems (Sternberg, 1875; Shaw and Kellerhals, 1982; Kodama, 1994a, 1994b; Attal and Lavé, 2006), although selective transport may be a factor in some environments (Brierley and Hickin, 1985; Paola et al., 1992; Ferguson et al., 1996; Hoey and Bluck, 1999).

We assessed bed-material attrition by a series of tumbler experiments. We collected five bed-

TABLE 3. PREDICTOR VARIABLES AND RESIDUAL CORRELATION

Variable	*P* values from Spearman correlation between residuals of regression and predictor variables: Regression data set (22 observations)	Regression data set and visual outliers (29 observations)
Area (km^2)*	0.89	0.94
Slope (m/m)*	0.47	0.33
Mean elevation (m)*	0.73	0.64
Maximum elevation (m)*	0.65	0.78
Minimum elevation (m)*	0.53	0.21
Relief (m)*	0.43	0.31
Mean precipitation (mm)†	0.42	0.62
Drainage density (km/km^2)§	0.63	0.05
Length of record (yr)#	0.82	0.21

Note: All variable values are given in supplementary Table DR6 (see text footnote 1).
*Calculated from U.S. Geological Survey National Elevation 1/3 arc-second data set, available at http://nationalmap.gov/index.html.
†Calculated from gridded (30 arc-second) mean annual precipitation estimates for the period 1971–2000 provided by the PRISM Climate Group, available at http://www.prism.oregonstate.edu.
§U.S. Geological Survey National Hydrography Data Set, 1:24,000 scale digital vector data obtained from http://nhd.usgs.gov/data.htm.
#Period represented by bed-material flux observations; complete information in supplementary Table DR6 (see text footnote 1).

material samples of ~10 L each from active gravel bars for each of five bedrock geologic provinces determined in the simplified classification of regional lithologies (Fig. 1; Tables DR8 and DR9 [see footnote 1]). An exception was that only four samples could be collected for the High Cascades province because of sparse bed material in streams draining this terrain. We excluded the Quaternary sedimentary unit from the attrition analysis since the clasts forming this unit presumably originate from the other five lithologic provinces. Samples were collected at sites where the contributing basin was solely composed of the targeted geologic province,[3] and each primary sample was from a separate basin. Collection sites were distributed throughout the range of the study area (Fig. 1) and had basin areas ranging from 3.4 km^2 to 1665 km^2 (median 65 km^2).

Multiple types of samples were prepared and analyzed (Table DR8 [see footnote 1]), but the standard sample introduced to the tumbler consisted of ~2000 g of gravel evenly divided among four 1/2φ size classes: 16–22.6 mm, 22.6–32 mm, 32–45 mm, and 45–64 mm. This distribution was a simplified approximation of subsurface bed material sampled from gravel bars within the study area.

Each sample was dried and weighed and then placed with 2 L of water into a Lortone QT 12 rotary tumbler. Each run was periodically halted, and the sample was drained, dried, and sieved. Size classes greater than 2 mm were individually weighed at 1/2φ intervals and then returned to the tumbler with 2 L of clean water. We did not retain sand (2 mm diameter) and finer grains, and the mass of these materials was included in the total mass loss of the experiment. For most trials, each sample was initially tumbled for 1 h followed by two 2 h runs and three 3 h runs, or else stopped when the sample had lost 25% of its initial mass (Table DR9 [see footnote 1]). For samples from the Coast Range sediments lithologic province, exceptionally rapid comminution required measurements at 5 min intervals. Time in the tumbler was converted to distance traveled by multiplying the 60 cm interior circumference of the tumbler by the 32 revolutions-per-minute speed of the tumbler, giving 1.152 km/h.

Following Sternberg (1875), a mass-loss coefficient (α) was determined for each sample on the basis of simple exponential linear regression of the mass measurements with distance (Fig. 6; Tables DR8 and DR9 [see footnote 1]). The relation takes the form of,

$$W_x = W_0 \cdot e^{(-\alpha x)}, \tag{4}$$

where W_x is the mass (in grams, g) of a particle after traveling distance x (km), W_0 is the initial particle mass (g), and α is the mass loss coefficient (km^{-1}). Higher α values signify higher rates of abrasion and conversion of bed material to material expected to be transported as part of the suspended load. While the resulting rates specifically pertain to the loss of gravel-size material, they are closely equivalent to bed-material mass loss (sizes greater than 0.5 mm) because the discarded wear products were dominantly fine sand, silt, and clay.

The multiple analyses of each geologic province indicate distinct rates of attrition among the lithologic types, while samples from the same terrains—even those from widely dispersed sites—are mutually consistent (Fig. 7A; Table DR8 [see footnote 1]). Splits of individual samples and samples including wider ranges of grain sizes gave similar results as the standard samples (Fig. 7B).

The hardest rocks—those losing mass at the lowest rates—were those from the High Cascades geologic province (Figs. 6 and 7). These are chiefly young unweathered basalts and basaltic andesites resulting from Quaternary Cascade Range volcanism. Of similar resistance to abrasion were the metamorphic Paleozoic and Mesozoic rocks of the Klamath terrane, mainly exposed in southwestern Oregon and northwest California. Slightly softer are the Tertiary volcanic rocks—chiefly basalts—of the Cascade and Coast Ranges. By far the softest rocks were the Tertiary sedimentary rocks of the Coast Range. These rocks lost more than half of their gravel-sized mass each kilometer (0.54 km^{-1}), a rate 80 times greater than rocks of the adjacent Klamath terrane, and as much as 1000 times greater than a sample of quartzite clasts (Fig. 7B). As discussed in more detail in subsequent sections, this discrepancy is probably the single most important factor explaining why rivers draining Coast Range sedimentary rocks have bedrock channels and long fluvial estuaries as they approach the Pacific Ocean.

Translating these experimental tumbler results into actual mass-loss rates along the rivers of our study area requires assuming that transport in the tumbler can be related to actual river transport distances. Some experiments have shown that the true particle travel distance in the tumbler may be less than half of that calculated from the tumbler circumference (Mikoŝ and Jaeggi, 1995). Consistent with this, several authors have suggested that experimental devices underestimate abrasion rates in rivers, as reviewed by Attal and Lavé (2009). Nevertheless, our tumbler-determined abrasion rates are higher than many other experimental studies and span similar values as determined in the few field cases where downstream size reduction can be confidently attributed to abrasion (Fig. 7B; Shaw and Kellerhals, 1982; Mikoŝ, 1994). Consequently, we use the results of the tumbler experiments without adjustment to approximate actual bed-material attrition rates, although this supposition remains unverified.

Regional Bed-Material Flux

Combining the bed-material yield estimates with our tumbler-derived attrition rates allows for spatially explicit predictions of bed-material flux in western Oregon and far northwestern California. Our approach was to calculate annual bed-material yield with Equation 3 for each 12 digit hydrologic unit code watershed ("HUC12"; description at http://water.usgs.gov/GIS/huc.html; accessed 5 June 2013) from the watershed boundary data set at http://datagateway.nrcs.usda.gov/ (accessed 17 May 2011). The median basin size for the 1042 HUC12 basins in our study area is 66 km^2, which is smaller than the 390 km^2 median area of the 22 basins of sediment yield observations underlying the bed-material yield estimates but well within the range of basin sizes with bed-material yield observations. The annual bed-material supply calculated in this manner for each HUC12 basin is assumed to enter the fluvial system (as derived from USGS 1/3 arc-second [10 m] resolution topographic data) at the basin outlet. Downstream from the entry point, the annual flux of bed material from the contributing basin was calculated on the basis of the lithologic composition of the basin, the lithologic-specific attrition rates derived from the tumbler experiments, and distance traveled. All of these calculations assume steady-state conditions with no net changes in bed-material storage along the hydrologic network.

By summing contributions from each basin and accounting for attrition, we calculated total annual bed-material flux at 1045 locations, providing spatially explicit predictions of bed-material flux for all streams draining one or more HUC12 watersheds (Fig. 8; Table DR10 [see footnote 1]). This analysis predicts a wide range of annual bed-material fluxes: as much as 572,000 t/yr just downstream of the confluence of the Rogue and Illinois Rivers, to less than 1000 t/yr at several basin outlets, particularly in the low-relief coastal plains flanking the Pacific Ocean, the broad volcanic uplands of parts of the High Cascade lithologic province, and within the lowlands of the Willamette Valley.

As expected from the empirical yield and attrition relations, topography and lithology strongly influence regional patterns of predicted bed-

[3]For a single sampling site (MFC-1 of Table DR8) of multiple upstream lithologic groups, a sample of Coast Range volcanic clasts was separated from a bar composed of both volcanic and sedimentary rocks.

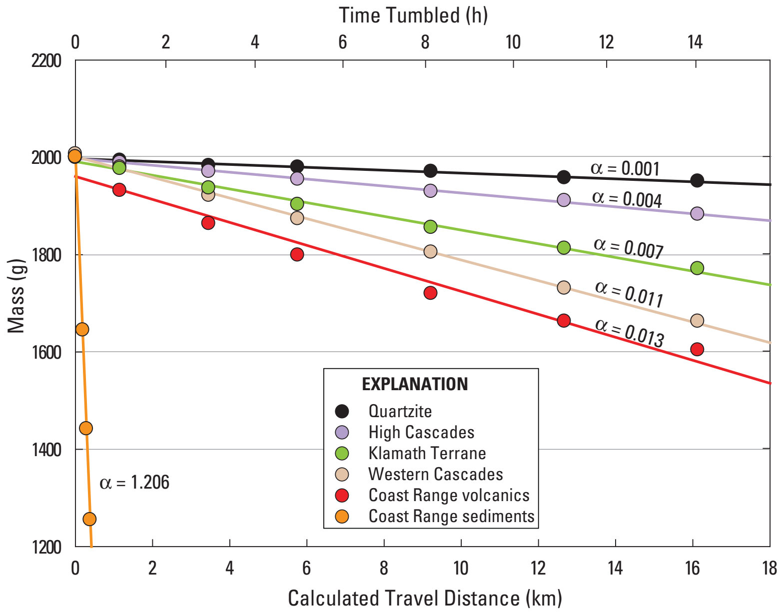

Figure 6. Plots of representative clast attrition experiments, showing one experiment and derived mass-loss coefficient, α, in units of km⁻¹, for each lithologic province. Complete tumbler experimental results are tabulated in supplementary Table DR9 (see text footnote 1).

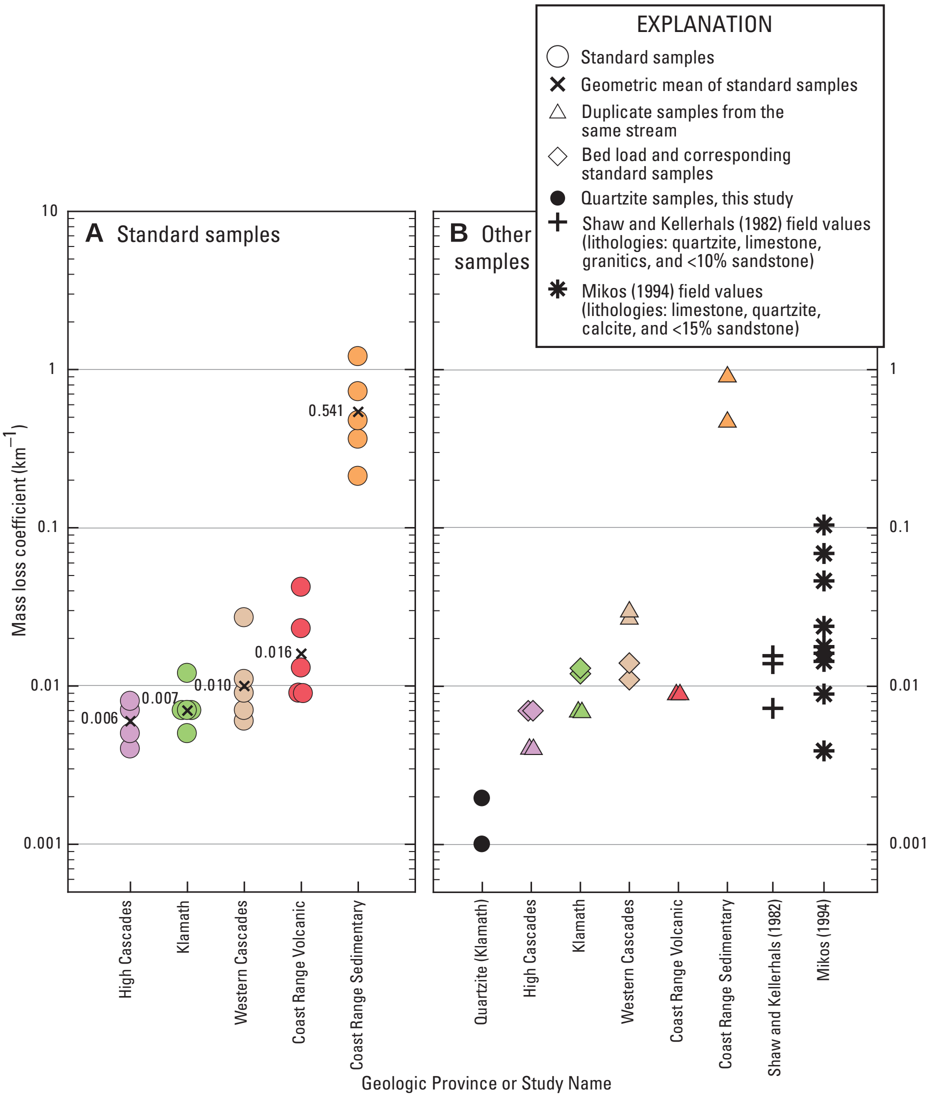

Figure 7. Summary results of attrition experiments from this study and other field-based measurements. Complete experimental results from analyses conducted in this study are tabulated in supplementary Table DR9 (see text footnote 1). (A) Results of standard-sample analyses for each lithologic terrain in the western Oregon study area, showing mean value used for bed-material flux calculations. (B) Results of duplicate and additional analyses (quartzite clasts and wider grain-size range for bed-material samples) in addition to the field-based clast attrition rates documented by Shaw and Kellerhals (1982) and Mikoŝ (1994). Standard and bed-material sample compositions are reported in supplementary Table DR8 (see text footnote 1).

Figure 8. Summary results of bed-material flux estimates for the western Oregon study area, with bed-material flux indicated by line width, based on calculations for 1045 HUC12 basins, as tabulated in supplementary Table DR10 (see text footnote 1). Results are shown for scenarios of no bed-material trapping by dams (maroon color), and assumed complete bed-material trapping by the 25 major dams in the study area (blue). Lithologic terrains are defined in Figure 1 and supplementary Table DR7 (see text footnote 1). Calculation nodes do not exactly correspond to dam locations, so effects of dams are generally attributed to next downstream calculation point.

material flux (Fig. 8). The greatest bed-material flux is predicted for the basins of southwestern Oregon and northern California, which drain the Klamath Mountains, reflecting the elevated yield from the Klamath terrane lithologic province, the high local slopes (mean slope = 0.40 ± 0.10 [m/m]), and the low attrition rate for Klamath terrane clasts. Relatively high bed-material transport is predicted for streams draining the Western Cascades and Coast Range volcanic lithologic provinces, also a result of the high basin slopes (0.29 ± 0.11 and 0.25 ± 0.17 [m/m], respectively) and the composition of materials, which are resistant to abrasion. Areas of low predicted bed-material flux include those drainage basins dominated by Quaternary sediments (mean slope 0.02) and the Coast Range sediments lithologic province, where bed-material yield from each basin is predicted to be high because of high average basin slopes (0.29 ± 0.11 [m/m]), but bed-material flux diminishes rapidly downstream because of exceptional attrition rates.

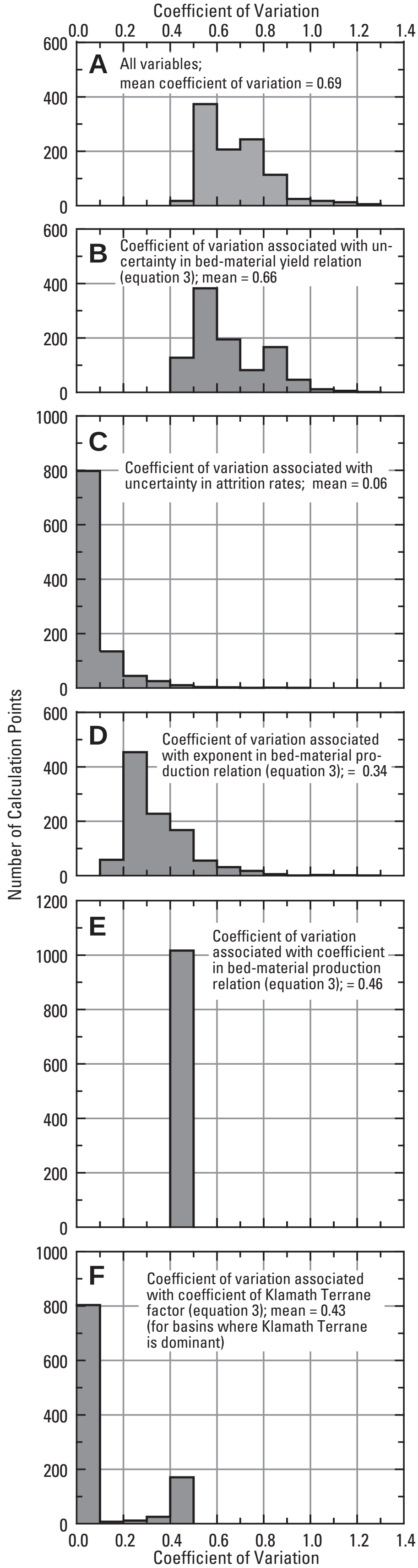

Figure 9. Results of Monte Carlo experiments investigating sources of uncertainty in bed-material flux calculations. Each case assessed 500 trials for each of 1045 calculation points. The primary conclusion from these experiments is that uncertainty in the bed-material yield relation is the major overall source of uncertainty in the sediment flux calculations. Results are summarized in supplementary Table DR11 (see text footnote 1). (A) Coupled yield and attrition model, showing distribution of total coefficient of variation associated with estimates of average annual bed-material transport at each calculation point. (B) Isolated analysis of coefficient of variation associated with the bed-material yield model of Equation 3. (C) Isolated analysis of coefficient of variation associated with the attrition estimates. (D–F) Analyses of the coefficient of variation associated with the individual parameters of the bed-material yield model of equation.

Uncertainty in Bed-Material Predictions

Uncertainty in these estimates derives from the combined uncertainty in the yield estimates and the attrition rates. On the basis of the estimated uncertainties of the sediment yield model (coefficients and exponents) and the mass-loss coefficients (from the multiple analyses), we conducted Monte Carlo experiments of 500 trials for each of several scenarios. Incorporating all the model uncertainties for bed-material yield and attrition rates, the coefficient of variation for the best-fit calculated bed-material flux at each of the 1045 calculation points ranged from 0.48 to 2.1, with an average of 0.69 (Fig. 9; Table DR11 [see footnote 1]). Separate Monte Carlo analyses of the influence of the uncertainty of the individual coefficients and exponents in the regression models show that the uncertainty in the bed-material yield model (Eq. 3) accounts for ~90% of total prediction uncertainty (Fig. 9), with the coefficient, exponent, and Klamath terrane factor (for basins where the Klamath terrane is the dominant lithology) all contributing about equally to the calculated uncertainty. This analysis nevertheless likely underestimates total uncertainty because of (1) our strengthening of the regression model by eliminating outliers and (2) employment of the unverified assumption that the tumbler-determined attrition rates directly correspond to rates along the rivers of the study.

Effects of Dams

The overall analysis does not account for bed-material trapped by dams. By assuming that each of 25 major dams in the western Oregon and northern California study area captures all bed-material entering upstream reservoirs, we can use the combined bed-material yield and comminution calculations to estimate the downstream effects of dams on bed-material flux (Fig. 8; Table DR10 [see footnote 1]). In total, bed-material supply is cut off from ~28% of the study area. Of the large basins, most affected is the Willamette River, where 34% of the basin no longer contributes bed material to the mainstem Willamette River at its mouth. However, the downstream effects on bed-material flux are even greater than this percentage would indicate; for example, our analysis indicates that dams have reduced the peak bed-material flux on the Willamette River by 64%—from 199,000 t/yr without dams just downstream of the Santiam River confluence, to 72,000 t/yr. Dams on the Coast Fork Willamette, Middle Fork Willamette, Santiam, and Clackamas Rivers have the largest apparent effects on overall bed-material fluxes. For the Willamette River, because of variable attrition rates and dam locations, the effects of dams diminish downstream, such that at the Willamette River confluence with the Columbia River, our calculations indicate that the bed-material flux has declined 58% as a consequence of impoundment, from 112,000 to 47,000 t/yr. Other large rivers, such as the Umpqua and Rogue Rivers, also have dams that trap bed material, but the overall effects become small downstream (Fig. 8). While this analysis shows regional patterns for large rivers of western Oregon, similar finer-scale analyses incorporating better information on locations and efficiency of bed-material trapping may be useful to examine effects of bed-material trapping for individual rivers and river reaches. Additionally, these calculations do not account for river incision or widening owing to reduced bed-material supply, which may partly compensate upstream supply loss.

Comparison with Other Measurements

The bed-material yield, attrition, and flux calculations lead to several testable predictions and comparisons. Because most of the dams have been in place several decades, most of the following comparisons employ flux estimates adjusted for trapping of bed material by the 25 major dams in the study area.

The most direct comparison would be with direct measurements of bed-material transport. Most such available measurements have been incorporated into the bed-material yield model (Table 2), but annual volumes of gravel bar replenishment at surveyed in-stream mining sites provide an indication of minimum transport rates. For the eight reaches for which such survey information is available (Table 4), volumes of gravel-bar deposition have ranged from 0.03 to 3.1 (median = 0.56) of the predicted bed-material transport for the surveyed reach (assuming a deposit density of 2.1 t/m^3). While this range is large, the South Fork Coquille River is the only one for which measured gravel deposition exceeded the predicted bed-material flux.

For Hunter Creek and the Chetco River, surveyed gravel recruitment volumes are not as complete as reports of mined volumes. For both of these alluvial reaches with extensive in-stream gravel mining, mined volumes over 9–20 yr have equated to ~1.1 times the predicted bed-material flux (Table 4). In particular for Hunter Creek, where there is little evidence of net incision or aggradation over the last several decades (Jones et al., 2011), this average removal volume may approach the bed-material flux into the reach, which in turn closely equates to the predicted flux from the yield and attrition routing. The situation may be similar for the Chetco River, but evidence of incision and bar-area loss since the 1970s (Wallick et al., 2010) indicates net bed-material loss that may partly coincide with the 2000–2008 time period for which mined gravel volumes slightly exceeded the predicted average annual flux. Summarizing the mining site measurements, aside from the South Fork Coquille River, the replenishment and mined volume measurements are consistent with the estimated bed-material fluxes.

Bed-material yield, in addition to fine sediment and solute loads, constitutes the total landscape denudation. From our bed-material

TABLE 4. SUMMARY OF GRAVEL BAR SURVEYS ASSOCIATED WITH IN-STREAM MINING SITES

	Observations from in-stream gravel mining operations								Bed-material flux estimates[#]			
River and reach	Number of sites*	Number of years	Period[†]	Average (t/yr)[§]	Maximum (t/yr)[§]	Maximum year	Minimum (t/yr)[§]	Minimum year	Best-fit model (t/yr)	16% quantile (t/yr)	84% quantile (t/yr)	Ratio of recruitment and extraction values to best-fit bed-material flux estimate ([t/yr]/[t/yr])
Reported recruitment												
Chetco	1	1	2006	93,678	N.D.**	N.D.	N.D.	N.D.	111,226	47,302	182,167	0.84
S. Fk. Coquille Broadbent	4–8	13	1996–2006; 2009	78,378	144,690	1999	28,640	2001	21,462	9524	35,319	3.65
Wilson	2	4	2006–2009	14,112	21,504	2007	10,395	2008	25,352	11,565	34,999	0.56
Kilchis	2	5	2004; 2006–2009	10,702	17,430	2006	5796	2008	23,426	12,336	31,199	0.46
Miami	1	3	2005–2007	3500	4998	2006	2604	2005	9949	5272	13,459	0.35
Nehalem	2	1	2009	30,996	N.D.	N.D.	N.D.	N.D.	34,692	17,521	47,118	0.89
South Umpqua Days Creek	1	5	2004–2006; 2008–2009	3800	80	2005	9210	2006	113,007	52,042	176,575	0.03
South Umpqua Roseburg	3–5	7	2003–2009	21,877	68,980	2006	6430	2009	165,172	70,838	274,246	0.13
Reported extraction												
Hunter	1–4	20	1991–2010	9561	24,793	1999	0	2001; 2003–2005	8552	3676	14,181	1.12
Chetco	4	9	2000–2008	123,054	188,954	2006	66,291	2008	111,226	47,302	182,167	1.11

Note: Recruitment and extraction values are summarized from Wallick et al. (2010, 2011) and Jones et al. (2011, 2012b, 2012c).
*For some reaches, the number of reporting sites varied during the assessed period of record.
[†]Analysis period based on completeness of survey records.
[§]Original volume measurements converted to tonnes on basis of 2.1 t/m^3.
[#]Flux values account for attrition and bed-material trapping by dams; 16th and 84th percentile values on basis of Monte Carlo analyses.
**N.D.—not determined or applicable.

yield analysis (in this case, ignoring bed-material trapping by dams), we can estimate vertical erosion rates associated with bed-material production for each HUC12 watershed. For the Coast Range and Klamath terrane lithologic provinces, these rates range from 0.05 to 0.13 mm/yr, assuming a rock density of 2.60 t/m^3 (Fig. DR2 [see footnote 1]). These values are ~10%–30% of regional uplift rates (Bierman et al., 2001; Heimsath et al., 2001; VanLaningham et al., 2006), a plausible value of bed-material production relative to total load if the Oregon Coast Range is in approximate steady state with respect to erosion and uplift, as proposed by Montgomery (2001). The areas of highest predicted erosion associated with bed-material production are in the Klamath Mountains in southwestern Oregon and northwestern California, the steeper parts of the Coast Range, and in the dissected Western Cascades.

The particle comminution modeling allows predictions of the mass of suspended load attributable to abrasion and the transformation of bed material to suspended load. The most complete suspended load records in the region are for the streamflow measurement site on the Umpqua River near Elkton (USGS streamflow station 14321000). This station accounts for 79% of the 12,103 km^2 basin, and it recorded an average suspended load 3,200,000 t/yr for the period 1956–1973 (Curtiss, 1975). By comparison, the predicted mass of bed-material loss due to attrition at that location—determined by subtracting the predicted bed-material flux (with dams) with attrition from that without attrition—is 533,000 t/yr; equivalent to 17% of the measured average annual suspended load.

The lithologic-dependent flux calculations also provide predictions of the lithologic composition of bed material at any location in the fluvial network. This prediction is challenging to test in the region because of the difficulty in distinguishing clasts among some lithologic provinces, especially those of the volcanic terrains. However, the distinctive sandstones and siltstones of the Coast Range sedimentary rocks allow partial evaluation. For the Umpqua River, we measured the abundance of sandstones and siltstones from samples of 400 surface clasts at each of 12 bars between river kilometer (RK) 175.5 and 46.7 (Wallick et al., 2011). The fraction of sedimentary rock clasts relative to all clast types ranged from 0.026 to 0.086 (0.038 ± 0.022). The predicted fraction of Coast Range sedimentary clasts for six flux calculation points between RK 166.6 and 56.2 ranges from 0.010 to 0.044 (0.030 ± 0.014). These values are not significantly different (two-sample *t*-test, $P > 0.05$), and both are much lower than the fraction of the contributing basin underlain by the Coast Range sedimentary rocks in this reach, which ranges from 0.12 to 0.25 (Wallick et al., 2011). For basins with more distinctive rock types, evaluation of clast abundance could be a strong test of this approach to estimating bed-material transport rates, and even serve as a basis for independent estimates of bed-material supply, flux, or attrition, as demonstrated by Mueller (2012) for gravel-bed rivers in the Rocky Mountains.

Although none of these evaluations of the bed-material flux predictions provides compelling confirmation of their accuracy, all are generally consistent. More systematic testing, particularly of bed-material flux rates and bed-material composition, would provide stronger evaluation of both the yield and attrition components of the analysis. Additionally, the Monte Carlo analyses indicate that overall improvement of the predictions would chiefly result from better statistical models of bed-material yield. Given the apparent importance of lithology, sufficient observations to discriminate yields from specific lithologic provinces in addition to the Klamath terrane would probably improve estimates.

DISCUSSION: BED-MATERIAL TRANSPORT AND CHANNEL GEOMORPHOLOGY

The bed-material transport results, although improvable and requiring more testing, do explain many aspects of regional and local channel morphology. For example, the divergent characters of the Rogue and Umpqua Rivers are explained by the lithologies that they drain. Additionally, the transport estimates clarify the distribution of alluvial and nonalluvial channels in western Oregon and correlate with measurable aspects of channel and valley-bottom morphology. More broadly, this examination of the settings and morphologies of the diverse channels draining western Oregon and northwestern California allows for general conclusions regarding bed-material supply and river form and processes, including the distribution of alluvial and nonalluvial channels and their key morphologic attributes.

The Umpqua and Rogue Rivers, a Tale of Two Lithologies

Comparison of the Umpqua and Rogue River basins illustrates how predicted bed-material flux is affected by variations in lithology and its resulting controls on bed-material yield and downstream comminution (Fig. 10). The Rogue River basin drains 13,390 km^2, slightly larger than the 12,103 km^2 of the Umpqua River. The basins have adjacent headwaters in the Cascade Range and flow through the Coast Range before emptying into the Pacific Ocean in southwestern Oregon. Although the headwaters of both basins are in the High Cascades lithologic province, and both have tributaries and headwater areas in the Western Cascade Range lithologic province, the Rogue River basin has much more of its area within the Klamath terrane (Fig. 1). By contrast, the lowermost 200 km of the Umpqua River flows mostly through rocks of the Coast Range sedimentary province (Figs. 1 and 10).

The predicted bed-material fluxes along these river corridors reflect these similarities and differences (Fig. 10). For both river systems, estimated bed-material flux increases downstream within the High Cascades and Western Cascades terrains, and annual transport rates climb substantially for both rivers upon entering the Klamath terrane lithologic province. For the South Fork Umpqua and main-stem Umpqua River system, the maximum estimated bed-material flux is 242,000 t/yr at RK 259 of the South Fork Umpqua River, with bed material mainly derived from the Klamath terrane (Fig. 10B). The predicted flux at a similar position on the Rogue River, which has not yet entered the Klamath terrane, is much lower—~40,000 t/yr (Fig. 10A). However, downstream, the patterns diverge in concert with the different rock types feeding into the two rivers. The Rogue River, which enters and then continues through Klamath terrane rocks, increases its bed-material flux to 572,000 t/yr just downstream of the confluence of the 2564 km^2 Illinois River at RK 43.8. The Illinois River, which is entirely within the Klamath terrane, contributes an estimated 273,000 t/yr at its mouth—constituting nearly half of the Rogue River's total. By contrast, the Umpqua River, which enters the Coast Range sediments at about RK 220, 37 km downstream of the location of peak bed-material flux, generally loses bed material downstream as attrition exceeds supply, declining to 78,000 t/yr at its entrance to the estuary at RK 44. The 961 km^2 Smith River, which is entirely within the Coast Range sedimentary province and enters the Umpqua River at RK 16, contributes only ~8000 t/yr of bed material to the lower Umpqua River.

These differences in predicted bed-material flux accord with river character. The lower Rogue River is floored and flanked by gravel bars to the Pacific Ocean (Fig. 2A). Tidal influence on the Rogue River is short, only extending 6.7 km inland from the Pacific, indicating that bed-material supply has kept pace with Holocene sea-level rise (Jones et al., 2012b). By contrast, the lower Umpqua River flows on bedrock with few gravel accumulations (Fig. 2C), until reaching tidal influence, which extends 44 km upstream (Wallick et al., 2011). The long fluvial estuary of the Umpqua River indicates that bed-

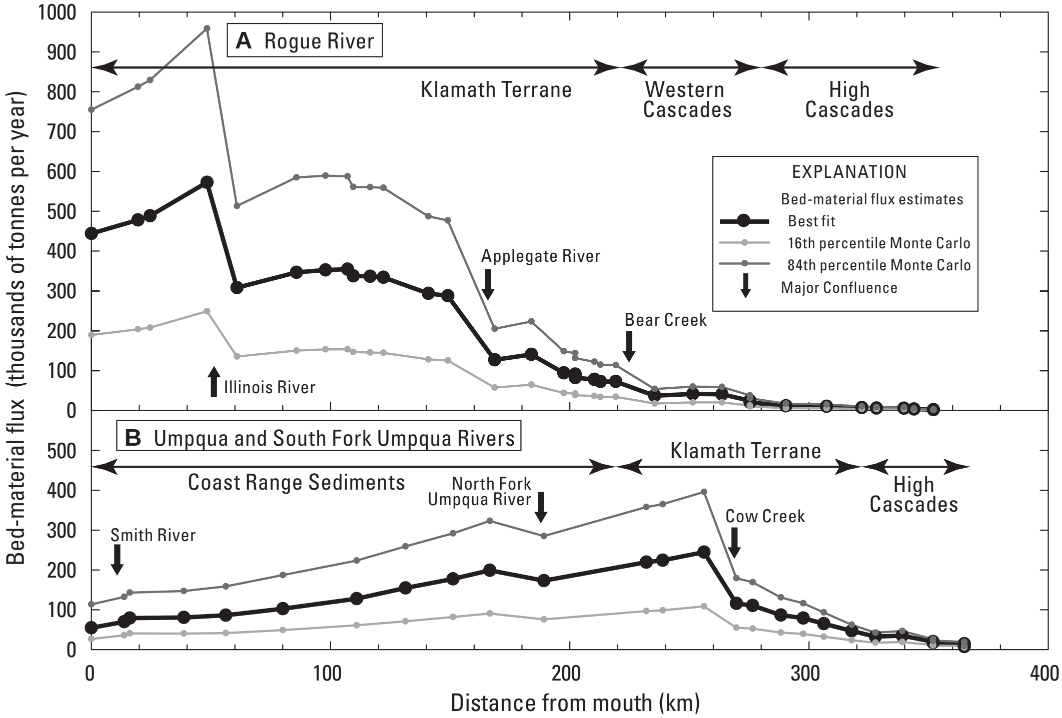

Figure 10. Estimated bed-material flux, assuming no trapping by dams, in relation to dominant surrounding geology for the (A) Rogue River (13,390 km²) and (B) Umpqua River (12,103 km²) basins of southwestern Oregon. This comparison emphasizes the importance of the distribution of rock types within the basin. The abundance of Coast Range sedimentary rocks susceptible to abrasion in the lower part of the Umpqua River basin results in substantial downstream decrease in bed-material flux. Supporting data are tabulated by HUC-12 basin in supplementary Table DR10 (see text footnote 1).

material accumulation has not kept up with Holocene sea-level rise, resulting in a partly drowned river valley near its Pacific Ocean confluence.

Bed-Material Flux and River Morphology

More broadly, the bed-material flux estimates allow further examination of the reach and site morphometry. For these correlations, we scaled the reach-specific best-fit bed-material flux estimates (adjusted for the presence of dams) by annual flow volume (Table 1). These values, essentially an annual bed-material concentration, were determined for calculation points representative of each analysis reach, typically near the downstream end (Table DR2 [see footnote 1]). To nondimensionalize this parameter, annual bed-material flux was converted to mineral volume by assuming a density of 2.6 t/m³. Because not all valley reaches had satisfactory streamflow measurement data, only 20 of the 24 reaches could be analyzed in this manner.[4]

Some reach characteristics correlate with local estimates of bed-material flux, while others do not. For example, neither bar-surface grain size nor, surprisingly, channel migration rate correlates with scaled bed-material transport (Figs. 11A and 11B). By contrast, scaled bed-material transport rate correlates strongly with both scaled bar area and *D**, but only for the alluvial reaches (Figs. 11C and 11D). In both cases, these relations bound most observations, with the alluvial reaches providing an upper bound to the bar-area measurements and a lower bound to the reach-averaged *D** values. These results parallel the morphometric relations shown in Figure 4, whereby bar area seemingly responds sensitively to bed-material flux, particularly for alluvial reaches.

Role of Geology and Physiography

As is known for many rivers, it is evident from this analysis that regional geology imparts an overriding influence on the character of gravel-bed rivers in western Oregon and northern California. This study clarifies that this influence comes about by two distinct avenues: its control on bed-material yield, and its control on downstream clast comminution.

Bed-Material Yield

Regionally, the accreted and uplifted Klamath terrane, affixed to western North America during the late Mesozoic Era and Early Tertiary Period, is an exceptional source of gravel bed material (Figs. 1, 8, and 10), contributing about four times the bed material per unit area relative to the other major lithologic provinces. Particularly high bed-material yields from the Klamath terrane likely are due to intense deformation associated with multiple episodes of Mesozoic and Early Tertiary accretion, predisposing these hard rocks to physical weathering and production of gravel-sized bed material. As a consequence of high bed-material yield rates, the rivers of southwest Oregon and northwest California have alluvial channels and high bed-material transport rates.

The Western Cascades also supply substantial bed material. This bed material is not as hard as that from the Klamath terrane, but the large area of the Western Cascades in conjunction with steep slopes result in significant bed-material production. Accordingly, the large rivers draining large areas of the Western Cascades, including the Coast and Middle Forks of the Willamette River, the McKenzie River, the Santiam River, the Molalla River, and the Clackamas River, are predominantly alluvial with gravel beds in their downstream reaches. It is bed material from this lithologic province that has been primarily trapped by dams in the study area that reduces bed-material volume in the main-stem Willamette River by as much as 64%.

These findings are consistent with many other studies documenting the control of lithology and physiography on sediment yield and channel morphology. Although most studies investigating physiographic and lithologic factors contributing to sediment yield or landscape denudation have

[4]Bed-material flux estimates for all basins could be scaled by other flow measures, such as the 0.5 annual exceedance flow, derived from regional regressions employed in StreamStats (http://water.usgs.gov/osw/streamstats), but these regressions for western Oregon rely on slope as a predictor variable and consequently are not independent of the bed-material flux estimates.

focused on total clastic yield (commonly based on measurements of suspended load), several point to slope and lithology as primary controls (Culling, 1960; Ahnert, 1970; Milliman and Syvitski, 1992; Summerfield and Hulton, 1994; O'Connor et al., 2003a; Aalto et al., 2006; Andrews and Antweiler, 2012; Mueller, 2012). Fewer studies have looked specifically at production of bed material; two recent studies that have evaluated bed-material production—Mueller (2012) and Andrews and Antweiler (2012)—both document strong lithologic influence on supply. In particular, Andrews and Antweiler (2012) showed that bedrock lithology, basin relief, and mean annual precipitation "are all highly significant predictors of mean annual sediment fluxes" for California coastal river basins. Mueller's (2012) analysis of Rocky Mountain rivers documented the strong influence of basin lithology on bed-material flux, with little influence of other basin factors such as slope, precipitation, drainage density, and basin relief.

Similar to the studies of Ahnert (1970), Pinet and Souriau (1988), Riebe et al. (2001), Aalto et al. (2006), and Mueller (2012), our analysis shows no additional explanatory power provided by employing mean precipitation as an additional predictor variable (Table 3; Fig. DR1 [see footnote 1]). In part this may be because precipitation strongly correlates to terrain factors such as elevation and slope in western Oregon (Daly et al., 2008), resulting in precipitation, slope, and bed-material yield all being highly correlated. This contrasts with Andrews and Antweiler's (2012) analysis of coastal California rivers, in which the best model of mean annual sediment yield was approximately linearly proportional to mean annual precipitation in addition to a strong dependence on basin relief.

Bed-Material Comminution

Our analysis indicates that bed-material flux and, consequently, channel morphology are strongly affected by particle comminution. This finding is amplified in the study area by the exceptionally low resistance of the Coast Range sediments to breakdown. For the Umpqua River, which has ~28% of the total basin underlain by the soft Coast Range sedimentary lithologic terrain, 94% of bed material erodes into sand and finer material during fluvial transport, substantially decreasing bed-material flux, resulting in bedrock channel boundaries, and boosting suspended sediment loads, and perhaps promoting floodplain building by enhanced overbank deposition. However, even for rivers predominantly draining rock types resistant to attrition, such as the Rogue River, particle comminution reduces calculated bed-material flux by more than half along the length of the river. In the western Oregon and northwestern California study area, the large disparity in attrition rates among the different rock types is a primary factor controlling regional river conditions.

The lithologic control of particle comminution and its effects on bed-material characteristics have been described by Krumbein (1941), Shaw and Kellerhals (1982), Kodama (1994a), and Attal and Lavé (2006, 2009), among others. Recent work has investigated related river network controls and implications (for example, Collins and Dunne, 1989; Pizzuto, 2005; Attal and Lavé, 2006; Sklar et al., 2006; Chatanantavet et al., 2010; Mueller, 2012). Together, these studies have shown, similar to this study, that in certain settings, lithologic control on particle attrition affects the bed-material flux and transport conditions, downstream patterns in bed-material size distribution, and the lithological distribution of bed material.

Our results also point to a little-made distinction between rock hardness with respect to its resistance to in-transit breakdown and its propensity to produce bed material. This is particularly the case for Klamath terrane rocks, which have significantly higher yield rates but comminution rates similar to other rock types in the region. The high yield rates of the Klamath terrane likely owe to pervasive fracturing and jointing that accompanied tectonic amalgamation, creating conditions of relatively weak hillslope-

Figure 11. Scatter plots of estimated bed-material flux in relation to selected morphologic and grain-size observations for alluvial, mixed-bed, and bedrock channels. Horizontal uncertainty bars for the flux values show the 16th and 84th percentile values from the Monte Carlo analyses. Flux values include effects of bed-material trapping by dams. Supporting data are tabulated in supplementary Tables DR2 and DR3 (see text footnote 1). (A) Median bar-surface grain size. Vertical uncertainty bars show standard deviation of multiple particle counts for reaches with five or more measurements, and entire range for reaches with fewer bar-surface grain-size measurements. The absence of vertical uncertainty bars indicates only a single particle size measurement for the reach. (B) Scaled migration rate. (C) Scaled bar area, showing significant positive correlation (and 95% confidence limits) with bed-material flux for alluvial channels. (D) D^* (= $[W \cdot S]/D_{50}$), a measure of local transport capacity relative to grain size, showing significant positive correlation with bed-material flux for alluvial channels.

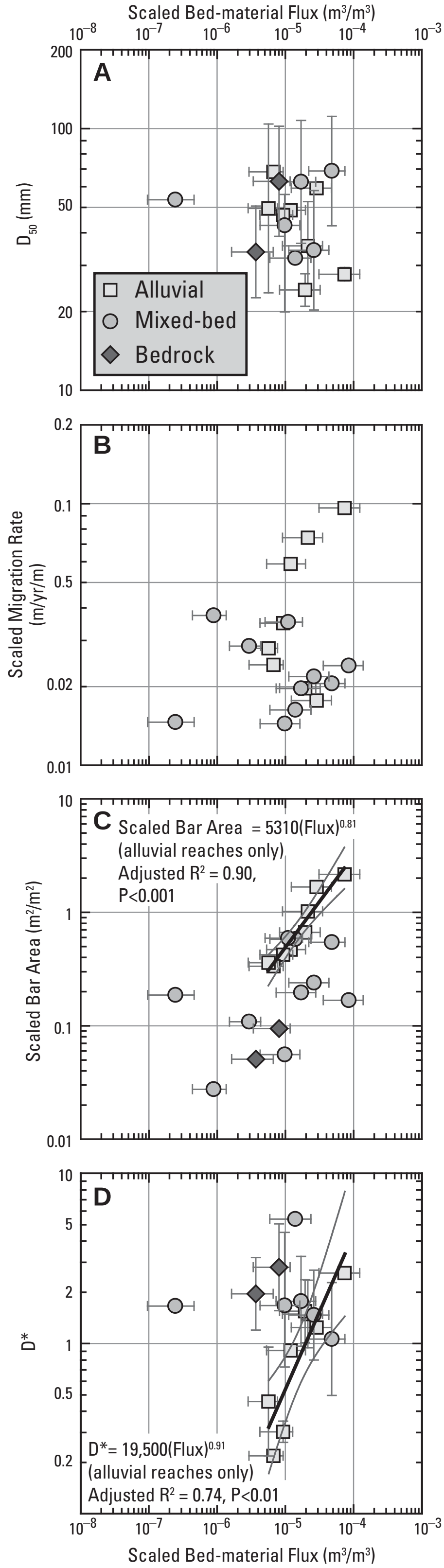

scale strength, whereas abrasion works slowly on mineral or grain boundaries within the small but coherent metasedimentary and metavolcanic clasts that have entered the channel. The Coast Range sediments behave oppositely; bed-material yield rates are unexceptional, but comminution rates are high for the weakly cemented siltstones and sandstones.

Alluvial and Nonalluvial Rivers

The geologic and physiographic factors on bed-material production and downstream comminution within the northern California and Oregon study area control the distribution of alluvial and nonalluvial channels. The distinction between channel types represents an important threshold in channel behavior (Howard, 1980; Lisle, 2012) affecting several geomorphic and ecological processes and conditions, and it has pragmatic implications for river management. Within the study area, alluvial channels have greater bar area, greater migration rates, and finer bar textures (Figs. 3 and 4). For alluvial channels, scaled bar area correlates positively with measures of transport capacity and estimated bed-material flux, whereas such correlations are not evident for nonalluvial reaches (Figs. 4C and 11C).

These differences accord with understanding of alluvial and bedrock channel behavior. The absence of a well-defined critical gradient separating nonalluvial from alluvial channels in the slope–drainage area plot (Fig. 4A) indicates that factors such as lithology or hydrology exert important influence (Montgomery et al., 1996). In this study area, lithology-controlled sediment supply and in-channel attrition are probably the primary factors obscuring the drainage area–slope threshold between alluvial and nonalluvial channels.

Lateral channel mobility for gravel-bed rivers requires bar building (Church, 1992), with rates of migration in part controlled by bar growth. Meander rates in general scale with bar area, regardless of channel type (Fig. 4C), but bar area strongly correlates with bed-material flux for only the alluvial reaches (Fig. 11C). The scaling factor of 0.81 in this relation indicates a nearly linear correspondence between scaled flux and scaled bar area. This latter observation is consistent with "sediment stage," an index of the volume of sediment in the active channel (Lisle, 2012), correlating with transport rates for alluvial channels (Lisle and Church, 2002). The absence of correlation of bar area and bed-material flux for the nonalluvial reaches is consistent with transport capacity exceeding supply. In nonalluvial reaches, we hypothesize that bars form primarily as a consequence of local hydraulic controls imposed by bedrock geometry and outcrops (Lisle, 1986, 2012; O'Connor et al., 1986).

Within the alluvial reaches, the positive correlation between D^*, the measure of local transport capacity relative to grain size, and scaled bar area (Fig. 4C) and the strong correlation between estimated bed-material flux and bar area (Fig. 11C) indicate that the alluvial channels in the study area have, to a certain extent, adjusted their morphometry to transport capacity. These results indicate "graded" channels as hypothesized by Mackin (1948) and quantified in Lane's (1955) equality relating flow, sediment flux, sediment caliber, and slope. The positive correlation between scaled flux and D^* also accords with observations that the threshold Shields values important for controlling channel morphology and bed texture increase with scaled bed-material transport rates and channel lability (Church, 2006); here, the scaling factor of 0.91 indicates the relation is nearly linear. The wide range of migration rates among alluvial reaches is in part influenced by bed-material flux (and its control on bar area), but some reaches, such as the Illinois River, are laterally confined by valley walls to the extent that migration rates are relatively low (Figs. 3 and 4).

The correlations for alluvial rivers between bed-material flux and (1) bar area and (2) D^* appear to be limiting relations bounding the observations from nonalluvial reaches (Figs. 11C and 11D). For the case of bar area, this indicates a systematic and maximum limiting relation between scaled bar area and bed-material flux, also consistent with the "sediment stage" concept of Lisle and Church (2002). The minimum limiting relation between bed-material flux and D^*, which scales with the Shields number, indicates relatively lower and systematically variable Shields number values for the alluvial rivers compared to higher and nonsystematic values for the nonalluvial reaches. Consequently, bed material is probably more frequently entrained in the nonalluvial reaches than in the alluvial reaches.

For nonalluvial rivers, our morphologic measurements and bed-material transport analyses indicate few systematic reach-scale patterns or correlations (Figs. 4 and 11), supporting the view that the distinction between alluvial and nonalluvial channels is an important threshold for fluvial systems. For nonalluvial reaches, it appears that local hydraulic and sediment supply conditions strongly influence morphologic characteristics and transport conditions, possibly indicated by the weak correlation between local slope and D_{50} (Fig. 4B). Little distinction is evident between reaches categorized as "mixed bed" and "bedrock" among the morphologic characteristics and relations.

Much of the recent research on bedrock and mixed-bed channels has been motivated by understanding the interactions between alluvial cover and channel incision in bedrock (reviewed by Turowski, 2012). The results here indicate that locations of alluvial and bedrock reaches, and consequently areas of bedrock incision and long-term landscape evolution, can be partly controlled by the spatial distribution of lithology and physiography and its effects on bed-material production, transport, and comminution down the fluvial network. As noted by Duvall et al. (2004), these types of lithologically controlled network effects on bed material can complicate the linkages among rock uplift, the distribution of bedrock and alluvial channels, channel incision, and resulting broad-scale channel morphologic characteristics such as profile concavity. For rivers such as the Umpqua River, where more than 90% of the bed material may disintegrate into suspended load, downstream river morphology and concavity may have little connection with basin-scale tectonic controls. These network effects are in addition to the local lithologic complications identified by VanLaningham et al. (2006) in their analysis of river concavity and morphology for the Oregon Coast Range, for which they concluded "inverting tectonic information from distributions of channel types and river profile concavity in tectonically active mountain belts depends on isolating lithologic and other variables independently."

CONCLUSIONS AND APPLICATIONS

Our studies were motivated by specific management issues pertaining to bed-material supply and its relation to channel morphology. Results are relevant to several aspects of these issues: Foremost, our coupled analysis of bed-material yield and in-channel attrition gives testable site-specific estimates of annual bed-material flux—a notoriously difficult-to-measure but important attribute for gravel-bed rivers. Although these estimates have large uncertainty, and annual values probably vary tremendously from year to year, they provide bounds for management of fluvial gravel resources. The analysis applied here also allows for estimating the effects of bed-material trapping by dams and other structures, thereby providing context for restoration strategies designed in consideration of bed-material transport. This approach is transferable to other regions where independent measures of bed-material yield can be obtained. Also, our results are also consistent with the idea that aspects of local bed-material flux may be estimated from the lithologic composition of the bed material (Mueller, 2012).

Our results also confirm the fundamental behavioral differences between alluvial and nonalluvial rivers. While our defining criteria directly relate to aspects of channel behavior—particularly the potential for reach-scale incision—the morphological relations also indicate other key distinctions with management implications. In particular for alluvial channels, bar area scales strongly with estimated bed-material transport rates, as well as transport capacity (as indicated by *D**). This observation suggests measurements of bar area can serve as both a predictor of bed-material supply, consistent with the "sediment stage" concept of Lisle and Church (2002), as well as a monitoring measure for reach-scale trends in bed-material flux. Other morphologic characteristics appear less sensitive. In particular, our measurements indicate few strong correlations between sediment supply and armoring and grain size, indicating that these attributes may be affected by clast attrition (Attal and Lavé, 2006) or reflect local conditions or recent history rather than reach-scale properties.

The strong correlations and limiting conditions shown by the relations among bed-material transport rates, local transport capacity, and bar area for alluvial rivers (Fig. 11) indicate that these relations could possibly be used to (1) estimate expected conditions for a system in which bed-material transport is perturbed or manipulated; (2) identify reaches that may be near alluvial-nonalluvial thresholds; and (3) identify systems that may be out of equilibrium with respect to channel form and bed-material transport rates. Additionally, the strong correlation between estimated bed-material flux and capacity for alluvial rivers (Fig. 11D) is consistent with the application of transport-capacity–based bed-material transport relations (Parker, 1990; Wilcock and Crowe, 2003; Pitlick et al., 2009; Wilcock et al., 2009) for estimating local bed-material transport rates in alluvial rivers as defined here.

The nonalluvial rivers in the study area, however, have few correlations among attributes or systematic patterns of behavior, thereby challenging management and monitoring. Although nonalluvial channels almost certainly have overall less sensitivity to perturbations in terms of overall channel morphology, specific morphologic features, such as in-channel gravel accumulations and flanking bars, may have elevated ecological importance because of their scarcity. However, our results give little insight as to how to predict changes in the texture and areal extent of bed-material accumulations as a consequence of changing transport conditions. For nonalluvial rivers, local conditions probably exert greater influence, and factors may vary considerably with the areal extent of alluvial cover (Hodge et al., 2011). Additionally for nonalluvial rivers, transport capacity equations for bed-material transport likely only provide maximum limiting transport estimates (Wallick et al., 2011), and better estimates of bed-material flux must derive from consideration of bed-material supply.

ACKNOWLEDGMENTS

This work was funded by the U.S. Army Corps of Engineers, Oregon Department of State Lands, and the U.S. Geological Survey. Charles Cannon, Danial Polette, Norman Buccola, Ester Duggan, Rachel Peavler, Tara Chestnut, Steve Sobieszczyck, Terrence Conlon, and Xavier Rodriquez Lloveras assisted with field measurements. Esther Duggan and Eric Stautberg assisted with the tumbler experiments. Tana Haluska and Charles Cannon provided geographic information systems assistance. Discussions with Gordon Grant, Janine Castro, Peter Klingeman, Joshua Roering, Thomas Lisle, Erich Mueller, Peter Wilcock, and John Pitlick helped shape many of the conclusions presented here. Geological Society of America reviewers, including Nicole Gasparini and Associate Editor Joel Pederson, improved the manuscript.

REFERENCES CITED

Aalto, R., Dunne, T., and Guyot, J.L., 2006, Geomorphic controls on Andean denudation rates: The Journal of Geology, v. 114, p. 85–99, doi:10.1086/498101.

Ahnert, F., 1970, Functional relationships between denudation, relief, and uplift in large, mid-latitude drainage basins: American Journal of Science, v. 268, p. 243–263, doi:10.2475/ajs.268.3.243.

Ambers, R.K., 2001, Using the sediment record in a western Oregon flood-control reservoir to assess the influence of storm history and logging on sediment yield: Journal of Hydrology (Amsterdam), v. 244, p. 181–200, doi:10.1016/S0022-1694(01)00331-6.

Andrews, E.D., and Antweiler, R.C., 2012, Sediment fluxes from California coastal rivers: The influences of climate, geology, and topography: The Journal of Geology, v. 120, no. 4, p. 349–366, doi:10.1086/665733.

Attal, M., and Lavé, J., 2006, Changes of bedload characteristics along the Marsyandi River (central Nepal): Implications for understanding hillslope sediment supply, sediment load evolution along fluvial networks, and denudation in active orogenic belts, *in* Willett, S.D., Hovius, N., Brandon, M.T., and Fisher, D.M., eds., Tectonics, Climate, and Landscape Evolution: Geological Society of America Special Paper 398, p. 143–172, doi:10.1130/2006.2398(09).

Attal, M., and Lavé, J., 2009, Pebble abrasion during fluvial transport: Experimental results and implications for the evolution of the sediment load along rivers: Journal of Geophysical Research, v. 114, F04023, doi:10.1029/2009JF001328.

Bierman, P.R., Clapp, E., Nichols, K., Gillespie, A., and Caffee, M.W., 2001, Ch. 5, Using cosmogenic nuclide measurements in sediments to understand background rates of erosion and sediment transport, *in* Harmon, R.S., and Doe, W.W., III, eds., Landscape Erosion and Evolution Modeling: New York, Kluwer Academic/Plenum Publishers, p. 89–116.

Brierley, G.J., and Hickin, E.J., 1985, The downstream gradation of particle sizes in the Squamish River, British Columbia: Earth Surface Processes and Landforms, v. 10, no. 6, p. 597–606, doi:10.1002/esp.3290100607.

Chatanantavet, P., and Parker, G., 2008, Experimental study of bedrock channel alluviation under varied sediment supply and hydraulic conditions: Water Resources Research, v. 44, W12446, doi:10.1029/2007WR006581.

Chatanantavet, P., Lajeunesse, E., Parker, G., Malverti, L., and Meunier, P., 2010, Physically based model of downstream fining in bedrock streams with lateral input: Water Resources Research, v. 46, W02518, doi:10.1029/2008WR007208

Church, M., 1992, Channel morphology and typology, *in* Calow, P., and Petts, G.E., eds., The Rivers Handbook: Oxford, UK, Blackwell, p. 126–143.

Church, M., 2002, Geomorphic thresholds in riverine landscapes: Freshwater Biology, v. 47, p. 541–557, doi:10.1046/j.1365-2427.2002.00919.x.

Church, M., 2006, Bed material transport and the morphology of alluvial river channels: Annual Review of Earth and Planetary Sciences, v. 34, p. 325–354, doi:10.1146/annurev.earth.33.092203.122721.

Collins, B.D., and Dunne, T., 1989, Gravel transport, gravel harvesting, and channel-bed degradation in rivers draining the southern Olympic Mountains, Washington, U.S.A.: Environmental Geology, v. 13, p. 213–224.

Culling, W.E.H., 1960, Analytical theory of erosion: The Journal of Geology, v. 68, p. 336–344, doi:10.1086/626663.

Curtiss, D.A., 1975, Sediment Yields of Streams in the Umpqua River Basin: U.S. Geological Survey Open-File Report, 1 plate with text.

Daly, C., Halbleib, M., Smith, J.I., Gibson, W.P., Doggett, M.K., Taylor, G.H., Curtis, J., and Pasteris, P.P., 2008, Physiographically sensitive mapping of climatological temperature and precipitation across the conterminous United States: International Journal of Climatology, v. 28, p. 2031–2064, doi:10.1002/joc.1688.

Duvall, A., Kirby, E., and Burbank, D., 2004, Tectonic and lithologic controls on bedrock channel profiles and processes in coastal California: Journal of Geophysical Research, v. 109, F03002, doi:10.1029/2003JF000086.

Dykaar, B.B., and Taylor, G.A., 2009, An Estimate of the Coarse Sediment Volume Trapped within Lost Creek Reservoir on the Rogue River: Santa Cruz, California, and Portland, Oregon, Ecohydrology West and U.S. Army Corps of Engineers, 44 p.

Ferguson, R., Hoey, T., Wathen, S., and Werritty, A., 1996, Field evidence for rapid downstream fining of river gravels through selective transport: Geology, v. 24, p. 179–182, doi:10.1130/0091-7613(1996)024<0179:FEFRDF>2.3.CO;2.

Ferrari, R.L., 2001, Henry Hagg Lake 2001 Survey: Denver, Colorado, U.S. Bureau of Reclamation, 17 p.

Finnegan, N.J., Sklar, L.S., and Fuller, T.K., 2007, Interplay of sediment supply, river incision, and channel morphology revealed by the transient evolution of an experimental bedrock channel: Journal of Geophysical Research, v. 112, no. F3, F03S11, 17 p., doi:10.1029/2006JF000569.

Gilbert, G.K., 1877, Report on the Geology of the Henry Mountains: Washington, D.C., U.S. Geographical and Geological Survey of the Rocky Mountain Region, 160 p.

Gilbert, G.K., 1914, The Transportation of Debris by Running Water: U.S. Geological Society Professional Paper 86, 263 p.

Gomez, B., 1991, Bedload transport: Earth-Science Reviews, v. 31, p. 89–132, doi:10.1016/0012-8252(91)90017-A.

Goode, J.R., and Wohl, E., 2010a, Substrate controls on the longitudinal profile of bedrock channels: Implications for reach-scale roughness: Journal of Geophysical Research, v. 115, F03018, doi:10.1029/2008JF001188.

Goode, J.R., and Wohl, E., 2010b, Coarse sediment transport in a bedrock channel with complex bed topography: Water Resources Research, v. 46, W11532, doi:10.1029/2009WR008135.

Grant, G.E. and Wolff, A.L, 1991, Long-term patterns of sediment transport after timber harvest, western Cascade Mountains, Oregon, USA, *in* Walling, D.E., and Peters, N., ed., Sediment and Stream Water Quality in a Changing Environment: Oxfordshire, U.K., Proceedings of the Vienna IAHS Symposium, International Association of Hydrological Sciences Publication No. 203, p. 31–40.

Heimsath, A.M., Dietrich, W.E., Nishiizumi, K., and Finkel, R.C., 2001, Stochastic processes of soil production and transport: Erosion rates, topographic variation and cosmogenic nuclides in the Oregon Coast Range: Earth Surface Processes and Landforms, v. 26, p. 531–552, doi:10.1002/esp.209.

Hodge, R.A., Hoey, T.B., and Sklar, L.S., 2011, Bed load transport in bedrock rivers: The role of sediment cover in grain entrainment, translation, and deposition: Journal of Geophysical Research, v. 116, F04028, doi: 10.1029/2011JF002032.

Hoey, T.B., and Bluck, B.J., 1999, Identifying the controls over downstream fining of river gravels: Journal of Sedimentary Research, v. 69, p. 40–50, doi:10.2110/jsr.69.40.

Hooke, R.L., 2000, Toward a uniform theory of clastic sediment yield in fluvial systems: Geological Society of America Bulletin, v. 112, p. 1778–1786, doi:10.1130/0016-7606(2000)112<1778:TAUTOC>2.0.CO;2.

Howard, A.D., 1980, Thresholds in river regimes, *in* Coates, D.R., and Vitek, J.D., eds., Thresholds in Geomorphology: London, George Allen and Unwin, p. 227–258.

Howard, A.D., 1998, Long profile development of bedrock channels: Interaction of weathering, mass wasting, bed erosion, and sediment transport, *in* Tinkler, J., and Wohl, E.E., eds., Rivers Over Rock: Fluvial Processes in Bedrock Channels: American Geophysical Union Geophysical Monograph 107, p. 297–319.

Howard, A.D., and Kerby, G., 1983, Channel changes in badlands: Geological Society of America Bulletin, v. 94, p. 739–752, doi:10.1130/0016-7606(1983)94<739:CCIB>2.0.CO;2.

Johnson, J.P., and Whipple, K.X., 2007, Feedbacks between erosion and sediment transport in experimental bedrock channels: Earth Surface Processes and Landforms, v. 32, p. 1048–1062, doi:10.1002/esp.1471.

Jones, K.L., Wallick, J.R., O’Connor, J.E., Keith, M.K., Mangano, J.F., and Risley, J.C., 2011, Preliminary Assessment of Channel Stability and Bed-Material Transport along Hunter Creek, Southwestern Oregon: U.S. Geological Survey Open-File Report 2011–1160, 41 p.

Jones, K.L., O’Connor, J.E., Keith, M.K., Mangano, J.F., and Wallick, J.R., 2012a, Preliminary Assessment of Channel Stability and Bed-Material Transport in the Rogue River Basin, Southwestern Oregon: U.S. Geological Survey Open-File Report 2011–1280, 96 p.

Jones, K.L., O’Connor, J.E., Keith, M.K., Mangano, J.F., and Wallick, J.R., 2012b, Preliminary Assessment of Channel Stability and Bed-Material Transport in the Coquille River Basin, Southwestern Oregon: U.S. Geological Survey Open-File Report 2012–1064, 84 p.

Jones, K.L., Keith, M.K., O’Connor, J.E., Mangano, J.F., and Wallick, J.R., 2012c, Preliminary Assessment of Channel Stability and Bed-Material Transport in the Tillamook Bay Tributaries and Nehalem River Basin, Northwestern Oregon: U.S. Geological Survey Open-File Report 2012–1187, 120 p.

Kodama, Y., 1994a, Downstream changes in the lithology and grain size of fluvial gravels, the Watarase River, Japan: Evidence of the role of abrasion in downstream fining: Journal of Sedimentary Research, v. 64A, p. 68–75.

Kodama, Y., 1994b, Experimental study of abrasion and its role in producing downstream fining in gravel-bed rivers: Journal of Sedimentary Research, v. 64A, p. 76–85, doi:10.2110/jsr.64.76.

Kondolf, G.M., Lisle, T.E., and Wolman, G.M., 2003, Bed sediment measurement, *in* Kondolf, G.M., and Piegay, H., eds., Tools in Fluvial Geomorphology: Chichester, UK, John Wiley & Sons, Inc., p. 347–396.

Krumbein, W.C., 1941, Measurement and geological significance of shape and roundness of sedimentary particles: Journal of Sedimentary Petrology, v. 11, p. 64–72.

Lane, E.W., 1955, Design of stable channels: Transactions of the American Society of Civil Engineers, v. 120, p. 1275–1279.

Lisle, T.E., 1986, Stabilization of a gravel channel by large streamside obstructions and bedrock bends, Jacoby Creek, northwestern California: Geological Society of America Bulletin, v. 97, p. 999–1011, doi:10.1130/0016-7606(1986)97<999:SOAGCB>2.0.CO;2.

Lisle, T.E., 2012, Transport capacity, bedrock exposure, and process domains, *in* Church, M., Biron, P.A., and Roy, A.G, eds., Gravel-Bed Rivers: Processes, Tools, Environments: Chichester, UK, John Wiley & Sons, p. 419–423, doi:10.1002/9781119952497.ch30.

Lisle, T.E., and Church, M., 2002, Sediment transport-storage relations for degrading, gravel bed channels: Water Resources Research, v. 38, p. 1219, doi:10.1029/2001WR001086.

Lisle, T.E., and Madej, M.A., 1992, Spatial variation in armouring in a channel with high sediment supply, *in* Billi, P., Hey, R.D., Thorne, C.R., and Tacconi, P., eds., Dynamics of Gravel-Bed Rivers: New York, John Wiley, p. 277–296.

Ludington, S., Moring, B.C., Miller, R.J., Stone, P.A., Bookstrom, A.A., Bedford, D.R., Evans, J.G., Haxel, G.A., Nutt, C.J., Flyn, K.S., and Hopkins, M.J., 2007, Western States: California, Nevada, Arizona, and Washington: U.S. Geological Survey Open-File Report 2005–1305, digital data.

Ma, L., Madin, I.P., Olson, K.V., Watzig, R.J., Wells, R.E., Niem, A.R., and Priest, G.R., 2009, Oregon Geologic Data Compilation [OGDC], Release 5 (Statewide): Portland, Oregon, Oregon Department of Geology and Mineral Industries, digital data, http://www.oregongeology.com/sub/ogdc/ (accessed August 2012).

Mackin, H.J., 1948, Concept of the graded river: Geological Society of America Bulletin, v. 59, p. 463–512, doi:10.1130/0016-7606(1948)59[463:COTGR]2.0.CO;2.

Massong, T.M., and Montgomery, D.R., 2000, Influence of sediment supply, lithology, and wood debris on the distribution of bedrock and alluvial channels: Geological Society of America Bulletin, v. 112, p. 591–599, doi:10.1130/0016-7606(2000)112<591:IOSSLA>2.0.CO;2.

MFG, Inc., Graham Mathews and Associates, and Alice Berg and Associates, 2006, Assessment of the Lower Smith River: Report prepared for County of Del Norte, Crescent City, California, 41 p.

Mikoŝ, M., 1994, The downstream fining of gravel-bed sediments in the Alpine Rhine River, *in* Ergenzinger, P., and Schmidt, K.H., eds., Dynamics and Geomorphology of Mountain Rivers: Berlin/Heidelberg, Springer, Lecture Notes in Earth Sciences, v. 52, p. 93–108.

Mikoŝ, M., and Jaeggi, M.N.R., 1995, Experiments on motion of sediment mixtures in a tumbling mill to study fluvial abrasion: Journal of Hydraulic Research, v. 33, p. 751–772, doi:10.1080/00221689509498550.

Milliman, J.D., and Syvitski, J.P.M., 1992, Geomorphic/tectonic controls of sediment discharge to the ocean—The importance of small mountainous rivers: The Journal of Geology, v. 100, p. 525–544, doi:10.1086/629606.

Montgomery, D.R., 2001, Slope distributions, threshold hillslopes, and steady-state topography: American Journal of Science, v. 301, p. 432–454, doi:10.2475/ajs.301.4-5.432.

Montgomery, D.R., and Buffington, J.M., 1997, Channel-reach morphology in mountain drainage basins: Geological Society of America Bulletin, v. 109, p. 596–611, doi:10.1130/0016-7606(1997)109<0596:CRMIMD>2.3.CO;2.

Montgomery, D.R., Abbe, T.B., Buffington, J.M., Peterson, N.P., Schmidt, K.M., and Stock, J.D., 1996, Distribution of bedrock and alluvial channels in forested mountain drainage basins: Letters to Nature, v. 381, p. 587–589, doi:10.1038/381587a0.

Mueller, E.R., 2012, Landscape Controls on Sediment Supply and Stream Channel Morpho-Dynamics in the Northern Rocky Mountains [Ph.D. thesis]: Boulder, Colorado, University of Colorado at Boulder, 187 p.

Newman, M.C., 1993, Regression analysis of log-transformed data: Statistical bias and its correction: Environmental Toxicology and Chemistry, v. 12, p. 1129–1133, doi:10.1002/etc.5620120618.

Nolan, K., and Janda, R., 1995, Impacts of Logging on Stream-Sediment Discharge in the Redwood Creek Basin, Northwestern California: U.S. Geological Survey Professional Paper 1454, p. L1–L8.

O’Connor, J.E., Webb, R.H., and Baker, V.R., 1986, Paleohydrology of pool-and-riffle pattern development: Boulder Creek, Utah: Geological Society of America Bulletin, v. 97, no. 4, p. 410–420, doi:10.1130/0016-7606(1986)97<410:POPPDB>2.0.CO;2.

O’Connor, J.E., Grant, G.E., and Haluska, T.L., 2003a, Overview of geology, hydrology, geomorphology, and sediment budget of the Deschutes River basin, Oregon, *in* O’Connor, J.E., and Grant, G.E.., ed., A Peculiar River—Geology, Geomorphology, and Hydrology of the Deschutes River, Oregon: Washington, D.C., American Geophysical Union Water Science and Application Series 7, p. 7–30.

O’Connor, J.E., Jones, M.A., and Haluska, T.L., 2003b, Flood plain and channel dynamics of the Quinault and Queets Rivers, Washington, USA: Geomorphology, v. 51, no. 1–3, p. 31–59, doi:10.1016/S0169-555X(02)00324-0.

PacifiCorp, 2004, Analysis of project effects on sediment transport and river geomorphology, chapter 6, *in* Klamath Hydroelectric Project, FERC 2082: Portland, Oregon, PacifiCorp, p. 6-1–6-170.

Paola, C., Parker, G., Seal, R., Sinha, S.K., Southard, J.B., and Wilcock, P.R., 1992, Downstream fining by selective deposition in a laboratory flume: Science, v. 258, p. 1757–1760, doi:10.1126/science.258.5089.1757.

Parker, G., 1990, Surface-based bedload transport relation for gravel rivers: Journal of Hydraulic Research, v. 28, p. 417–436, doi:10.1080/00221689009499058.

Pinet, P., and Souriau, M., 1988, Continental erosion and large-scale relief: Tectonics, v. 7, p. 563–582, doi:10.1029/TC007i003p00563.

Pitlick, J., Cui, Y., and Wilcock, P., 2009, Manual for Computing Bed Load Transport Using BAGS (Bedload Assessment for Gravel-Bed Streams) Software: U.S. Department of Agriculture, Forest Service, Rocky Mountain Research Station, General Technical Report RMRS-GTR-223, 45 p.

Pizzuto, J.E., 2005, Numerical modeling of alluvial landforms, *in* Kondolf, G.M., and Piegay, H., eds., Tools in Fluvial Geomorphology: Chichester, UK, John Wiley & Sons, p. 577–595.

Richardson, K., and Carling, P.A., 2005, A Typology of Sculpted Forms in Open Bedrock Channels: Geological Society of America Special Paper 392, 108 p., doi:10.1130/0-8137-2392-2.1.

Riebe, C.S., Kirchner, J.W., Granger, D.E., and Finkel, R.C., 2001, Minimal climatic control on erosion rates in the Sierra Nevada, California: Geology, v. 29, p. 447–450, doi:10.1130/0091-7613(2001)029<0447:MCCOER>2.0.CO;2.

Shaw, J., and Kellerhals, R., 1982, The Composition of Recent Alluvial Gravels in Alberta River Beds: Alberta Research Council Bulletin 41, 151 p.

Sklar, L.S., and Dietrich, W.E., 2001, Sediment and rock strength controls on river incision into bedrock: Geology, v. 29, p. 1087–1090, doi:10.1130/0091-7613(2001)029<1087:SARSCO>2.0.CO;2.

Sklar, L.S., Dietrich, W.E., Foufoula-Georgiou, E., Lashmeres, B., and Bellugi, D., 2006, Do gravel bed river size distributions record channel network structure?: Water Resources Research, v. 42, p. 22, doi:10.1029/2006WR005035.

Stanford, J.A., and Ward, J.V., 1993, An ecosystem perspective of alluvial rivers: Connectivity and the hyporheic corridor: Journal of the North American Benthological Society, v. 12, p. 48–60, doi:10.2307/1467685.

Stednick, J.D., 2008, The new Alsea watershed study, *in* Stednick, J.D., ed., Hydrological and Biological Responses to Forest Practices, Volume 199: Berlin, Springer, p. 115–121.

Sternberg, H., 1875, Untersuchungen uber Langen-und Querprofil geschiebefuhrender Flusse: Zeitschrift für Bauwesen, v. 25, p. 483–506.

Stillwater Sciences, 2000, North Umpqua Cooperative Watershed Analysis, Technical Appendix to the Synthesis Report, Appendix 2–1, Sediment Budget for the North Umpqua River Basin: Prepared for PacifiCorp, North Umpqua Hydroelectric Project, FERC Project No. 1927: Portland, Oregon, Stillwater Sciences, 113 p.

Stillwater Sciences, 2006, Technical Memorandum, Gravel Augmentation Pulse Experiment—August 2006 Reconnaissance Survey: Arcata, California, Stillwater Sciences, 3 p.

Summerfield, M.A., and Hulton, N.J., 1994, Natural controls of fluvial denudation rates in major world drainage basins: Journal of Geophysical Research, v. 99, p. 13,871–13,883, doi:10.1029/94JB00715.

Tetratech, 2009, Upper North Santiam River Gravel Augmentation Study—Final Report: Portland, Oregon, prepared for North Santiam Watershed Council and U.S. Army Corps of Engineers, Portland District, 84 p.

Tinkler, J., and Wohl, E.E., eds., 1998, Rivers Over Rock: Fluvial Processes in Bedrock Channels: American Geophysical Union Geophysical Monograph 107, 323 p.

Turowski, J.M., 2012, Semi-alluvial channels and sediment-flux–driven bedrock erosion, *in* Church, M., Biron, P.M., and Roy, G., eds., Gravel-Bed Rivers: Processes, Tools, Environments: Chichester, UK, John Wiley & Sons, Ltd., p. 401–417, doi:10.1002/9781119952497.ch29.

Turowski, J.M., Lague, D., and Hovius, N., 2007, Cover effect in bedrock abrasion: A new derivation and its implications for the modeling of bedrock channel morphology: Journal of Geophysical Research, v. 112, F04006, doi:10.1029/2006JF000697.

Turowski, J.M., Hovius, N., Meng-Long, H., Lague, D., and Men-Chiang, C., 2008a, Distribution of erosion across bedrock channels: Earth Surface Processes and Landforms, v. 33, no. 3, p. 353–363, doi:10.1002/esp.1559.

Turowski, J.M., Hovius, N., Wilson, A., and Horng, M.-J., 2008b, Hydraulic geometry, river sediment and the definition of bedrock channels: Geomorphology, v. 99, p. 26–38, doi:10.1016/j.geomorph.2007.10.001.

VanLaningham, S., Meigs, A., and Goldfinger, C., 2006, The effects of rock uplift and rock resistance on river morphology in a subduction zone forearc, Oregon, USA: Earth Surface Processes and Landforms, v. 31, p. 1257–1279, doi:10.1002/esp.1326.

Wallick, J.R., Anderson, S.W., Cannon, C., and O'Connor, J.E., 2010, Channel Change and Bed-Material Transport in the Lower Chetco River, Oregon: U.S. Geological Survey Scientific Investigations Report 2010–5065, 68 p.

Wallick, J.R., O'Connor, J.E., Anderson, S.W., Keith, M.K., Cannon, C., and Risley, J.C., 2011, Channel Change and Bed-Material Transport in the Umpqua River Basin, Oregon: U.S. Geological Survey Scientific Investigations Report 2011–5041, 112 p.

Wampler, P.J., 2004, Contrasting Styles of Geomorphic Response to Climatic, Anthropogenic, and Fluvial Changes across Modern to Millennial Time Scales, Clackamas River Oregon [Ph.D. dissertation]: Corvallis, Oregon, Oregon State University, 398 p.

Whipple, K.X., 2004, Bedrock rivers and the geomorphology of active orogens: Annual Review of Earth and Planetary Sciences, v. 32, p. 151–185, doi:10.1146/annurev.earth.32.101802.120356.

Whipple, K.X., Hancock, G.S., and Anderson, R.S., 2000, River incision into bedrock: Mechanics and relative efficacy of plucking, abrasion, and cavitation: Geological Society of America Bulletin, v. 112, p. 490–503, doi:10.1130/0016-7606(2000)112<490:RIIBMA>2.0.CO;2.

Wilcock, P., and Crowe, J., 2003, Surface-based transport model for mixed-size sediment: Journal of Hydraulic Engineering, v. 129, p. 120–128, doi:10.1061/(ASCE)0733-9429(2003)129:2(120).

Wilcock, P., Pitlick, J., and Cui, Y., 2009, Sediment Transport Primer Estimating Bed-Material Transport in Gravel-Bed Rivers: U.S. Department of Agriculture, Forest Service, Rocky Mountain Research Station, General Technical Report RMRS-GTR-226, 78 p.

Wohl, E.E., 1998, Bedrock channel morphology in relation to erosional processes, *in* Tinkler, J., and Wohl, E.E., eds., River Over Rock: Fluvial Processes in Bedrock Channels: American Geophysical Union Geophysical Monograph 107, p. 133–151.

Wohl, E.E., and Merritt, D.M., 2001, Bedrock channel morphology: Geological Society of America Bulletin, v. 113, p. 1205–1212, doi:10.1130/0016-7606(2001)113<1205:BCM>2.0.CO;2.

Yarnell, S.M., Mount, J.F., and Larsen, E.W., 2006, The influence of relative sediment supply on riverine habitat heterogeneity: Geomorphology, v. 80, p. 310–324, doi:10.1016/j.geomorph.2006.03.005.

Science Editor: Christian Koeberl
Associate Editor: Joel Pederson

Manuscript Received 9 October 2012
Revised Manuscript Received 9 July 2013
Manuscript Accepted 20 November 2013

Printed in the USA